የኢፌዲሪ የቴክኒክና ሙያ ስልጠና ኢንስቲትዩት
FDRE TECHNICAL & VOCATIONAL TRAINING INSTITUTE

TECHNICAL AND VOCATIONAL TRAINING INSTITUTE

(TVTI)

School of Graduate Studies

FACULTY OF ELECTRICAL AND ELECTRONICS TECHNOLOGY AND INFORMATION AND COMMUNICATION TECHNOLOGY (DEPARTMENT OF ELECTRICAL AND ELECTRONICS TECHNOLOGY)

Speed Control of Permanent Magnet Brushless DC (BLDC) Motors using Model Reference Adaptive Control (MRAC)

MSc Thesis for the Partial Fulfillment of

Master of Science (MSc) in Electrical Automation and Control Technology Management

By

Said Eshetu (TTMR/193/16)

Advisor

Dr. **YOHANNES HAILEMESKEL**

MAR 2026

Addis Ababa, Ethiopia



የኢፌዲሪ የቴክኒክና ሙያ ስልጠና ኢንስቲትዩት
FDRE TECHNICAL & VOCATIONAL TRAINING INSTITUTE

Speed Control of Permanent Magnet Brushless DC (BLDC) Motors using Model Reference Adaptive Control (MRAC)

A Thesis submitted to

Technical and Vocational Training Institute (TVTI)

Faculty of Electrical and Electronics Technology and Information and Communication Technology

(Department of Electrical and Electronics Technology)

In partial fulfillment for the Degree

Master of Science in Electrical Automation and Control Technology Management

Advisor

Dr. YOHANNES HAILEMESKEL

MAR 2026

Addis Ababa, Ethiopia

DECLARATION

The research thesis title Speed Control of Permanent Magnet Brushless (BLDC) DC Motors Using Model Reference Adaptive Control (MRAC) submitted in partial fulfillment of the Master of Science degree requirements at Federal Technical and Vocational Training Institute is my original work. This thesis represents my own independent research, conducted under the guidance of my advisor Dr. Yohannes Hailemeskel. I further declare that the research work that is included in this thesis is based on my own investigations, with proper acknowledgement given to all sources of information and assistance received. The data, and all sources of information and assistance have been properly acknowledged and cited. The author declares the accuracy of the data, experimental results, figures, and tables presented in the thesis, ensuring they have not been falsified or manipulated. The author acknowledges the seriousness of plagiarism and asserts that proper citation and referencing have been employed..

Candidate Seid Eshetu **Signature _____**

Place: Federal Technical and Vocational Training Institute, Addis Ababa.

Date of Submission _____

.

This thesis has been submitted for examination with my approval as a TVTI advisor

Dr. Yohannes Hailemeskel	_____	_____
Advisor Name	**Signature**	**Date**



የኢፌዲሪ የቴክኒክና ሙያ ስልጠና ኢንስቲትዩት
FDRE TECHNICAL & VOCATIONAL TRAINING INSTITUTE

TECHNICAL AND VOCATIONAL TRAINING INSTITUTE (TVTI)
FACULTY OF ELECTRICAL AND ELECTRONICS TECHNOLOGY AND INFORMATION AND COMMUNICATION TECHNOLOGY
(DEPARTMENT OF ELECTRICAL AND ELECTRONICS TECHNOLOGY

Thesis on

Speed Control of Permanent Magnet Brushless DC (BLDC) Motors using Model Reference Adaptive Control (MRAC)

By

Seid Eshetu **(TTMR 193/16)**

APPROVED BY THESIS ADVISORY COMMITTE

Name of the advisor	**signature**	**date**
Dr. Yohannes Hailemeskel	----------	----------
Name of the Examiner, internal	**signature**	**date**
----------	----------	----------
Name of the Examiner external	**signature**	**date**
----------	----------	----------

Acknowledgment

First, I would like to give the greatest thanks to the Almighty God who helped me in all directions. Also, I would like to express my sincere gratitude to my advisors, Dr. Yohannes Hailemeskel , for their invaluable guidance, support, and encouragement throughout this research. Their expertise, feedback, and insightful suggestions have been instrumental in shaping the direction and quality of my work. I am truly grateful for their unwavering commitment and dedication. I would like to express my sincere gratitude to the Department of Electrical and Electronics Technology staff for their support, guidance, and mentorship throughout the completion of thesis. Additionally, I would like to acknowledge the financial and instrumental support provided by the Federal Technical & Vocational Training Institute. Their generous funding has enabled me to carry out this research and covering expenses of research-related costs. Finally, but just as importantly, I want to sincerely thank my family and friends for their constant support, understanding, and encouragement during this study journey.

Abstract

Permanent Magnet Brushless DC (BLDC) motors is the most used industrial applications such as robotics, aerospace, and home appliances due to their high efficiency, compact size, and low maintenance requirements. The primary aim of this thesis was to Speed Control of Permanent Magnet Brushless DC(PMBLDC) Motors Using Model Reference Adaptive Control(MRAC). This thesis was the system for designing a MRAC with Lyapunov stability system nd MIT rule for the speed control of a Permanent Magnet Brushless DC(PMBLDC) motor using MATLAB/ Simulink.. The performance of each system was evaluated based on transient characteristics, including rise time, settling time, and overshoot, using a reference speed of 4000 rpm. All control strategies are designed and evaluated in MATLAB/Simulink with a reference speed of 4000 rpm under load torque disturbances ranging from 0.01 N·m to 100 N·m. The Simulation results show that the PID controller achieves a rise time of 0.2146 s and a settling time of 1.8014sec, but exhibits significant overshoot of 31.3514% under a 0.08 N·m load torque and under Load Torque 100N.m the riseing time 0.2389 sec ,settling time 01.8243 and over shoot 28.7676 % , The large ovrshoot it limited**;** sensitive to parameter changes and load variations. The MRAC with MIT rule , seady state error zero and the zero overshoot with a rise time of 0.439 s and a settling time 1.40 sec under heavy load conditions. MRAC with Lyapunov stability methode demonstrates superior performance by guaranteeing closed-loop stability, achieving zero overshoot, steady-state error, and smooth transient response, with rise times of 0.85– 0.90 s and settling times of 1.41–1.49 s even under a 100 N·m load torque.The error decay is smooth and non-oscillatory, verifying the method's effectiveness in handling system uncertainties. MRAC with Lyapunov stability provides enhanced robustness and stability compared to conventional PID controller . The MRAC with Lypaunov stability controllers, making it a suitable solution for high-performance PMBLDC motor speed control applications and the most reliable strategy for high-performance industrial applications due to its guaranteed stability and excellent damping.

Keywords: BLDC motor , MRAC, MIT rule, Lyapunov stability , Propertional integral derivative controller.

Table of Contents

DECLARATION i
Acknowledgment iii
Abstract iv
List of figure vii
List of tables viii
LIST OF ACRONYMS ix
LIST OF SYMBOL ix
Line resistance of the winding, ... x
CHAPTER ONE 1
INTRODUCTION 1
1.1 Background of the study 1
1.2 Statement of the problem 3
1.3 Objectives of the thesis 4
1.3.1 General objectives 4
1.4 Scope of the study 4
1.5 Significance of the Study 4
1.6 Limitation of the study 5
CHAPTER TWO 6
LITERATURE REVIEW 6
2.1. Related work of Literature review 6
2.2 Summary of Literature Review 14
CHAPTER THREE 15
METHODOLOGY 15
3.1 Chapter overview 15
3.2 Material 15
3.3 Methodology 15
3.4 Mathematic Modeling of permanent magnet brushless DC Motor 17
3.5 Basic Structure of Permanent Magnet Brushless DC (PMBLDC) Motors 17
3.5 .1 The Cores of Stator 18
3.5.2 winding 19
3.5.3 permanent Magnet Rotor 20
3.5.4 Position Sensor 21

3.6 Differential Equation Model 21
3.6.1 Transfer Functions 32
3.6.2 Stability analysis Permeant magnet brushless DC motor 38
CHAPTER FOUR 44
DESIGN OF CONTROLLER 44
4.1 Chapter Overview 44
4.2 Controller Design 44
4.2.1 Adaptive Control Scheme 44
4.2.2 Model Reference Adaptive Controller 44
4.2.3 Design Model Reference Adaptive Control with MIT Rule 45
Figure 4.2 The (MRAC) with the MIT rule. 49
4.2.4 Design of a Model Reference Adaptive Controller Using the Lyapunov Stability Method 49
4.2.5 Proportional-Integral-Derivative (PID) controller 53
CHAPTER FIVE 55
RESULT AND DISCUSSION 55
5.1 Chapter Overview 55
5.2 Simulation Parameters 56
5.3 The Performance Analysis 58
5. 3.1 Proportional- integral -derivative (PID) controller 58
5.3.2 MRAC with MIT Rule Result 63
5.3.3 Model Reference Adaptive control with Lyapunov stability Result 67
5.3.4 Comparison Between PID Controller and Lyapunov-Based MRAC 73
CHAPTER SIX 74
CONCLUSIONS AND RECOMMENDATIONS 74
6.1 Conclusions 74
6.2 Recommendations 75
Reference 76

List of figure

Figure 3.1 Thesis flow chart 16
Figure 3.2: Cross-sectional view of a Permanent Magnet Brushless DC (PMBLDC) motor, ... 19
Figure 3.3 permanet Magnet breshless Dc motor Schematic diagram 23
Figure 3.4: Permanent magnet flux linkage 25
Figure 3.5 The Rotor the magnetic of circuit. [27] 27
Figure 3.6 presents the phase same character B (**θ**), $\boldsymbol{fA}$ (**θ**) [27] 29
Figure 0.7 The same circuit Permanet Magnet Brushless Dc motor 29
Figure 3.8: The equal circuit a brushless dc motor during operation 34
Figure 3.9: Configuration of a brushless dc motor operating under no-load conditions 35
Figure 3.10: The Speed response of the BLDC motor 37
Figure 3.11 The Brshless dc motor with load torque. 37
figure 3.12 With out controller permanent Magnet Brushless DC motor response 43
Figure 4.1 Model Reference adaptive control 45
Figure 4.3 MRAC with Lyapunov Stability Method. 53
Figure 4.4 : Block diagram of a process control PID controller. 54
Figure 5. 1 Response model reference for an input reference of 4000rpm 57
Figure 5.2 Simulink model block PID controller input reference 4000rpm 58
Figure 5.3 Internal PID controller of simulation model 59
Figure 5.4 Simulink result PID controller Load Torque 0.08 N.m input reference 4000rpm 60
Figure 5.5 Simulink result Load Torque 100N.m input reference 4000rpm 61
Figure 5.6 Track error signal PID controller 62
Figure 5.7 The MATLAB/Simulink block diagram of MRAC with MIT rule 63
Figure 5.8 Response of PMBLDC Motor Load Torque 0.05 N·m MIT Rule input reference 4000rpm. 64
Figure 5.9 Response of the system under Load Torque 0.08 N.m conditions using MIT rule input reference 4000rpm. 65
Figure 5.10 Response of Load Torque 100 N.m MRAC with MIT Rule input reference 4000rpm 66
Figure 5.11 MATALB/Simulink model system block MRAC- Lyapunov stability Method 67
Figure 5.12 Simulink result Lyapunlov no Load torque input reference 4000rpm 68
Figure 5.13 Simulink result Lyapunov suitability Load Torque 0.01 input reference 4000rpm .. 69
Figure 5.14 Simulink result Lyapunov Load torque 0.08 input reference 4000rpm 70
Figure 5.14. Simulink result of Lyapunov stability the Load Torque 100N.m input reference 4000rpm. 71
Figure 5.15 Track Error for a Lyapunov-based MRAC speed control of a PMBLDC motor 72

List of tables

Table 0.2 Parameter of Permanent Magnet Brushless Dc Motor 38
Table 5.1 Simulation parameter of the Permeant magnet brushless Dc motor..... 56

LIST OF ACRONYMS

CD-RW	Compact Disc, Rewriteable Direct
BLDC	Brushless DC
NdFeB	Neodymium(Nd)iron(Fe) and boron(B)
DC	Direct current
PMBLDM	Permanente magnate brushed DC motor
MRAC	Model Reference Adaptive control
MIT	Massachusetts Institute of Technology rule
PWM	Pulse Width Modulation
VVS	Variable Voltage Source
AMC	American Motor Car Company
EMI	Electromagnetic Interference
EMF	Electromotive Force
FLC	Fuzzy Logic Controller
IM	Induction Motor
MOSFET	Metal Oxide Silicon Field Effect Transistor
PID	Proportional Integral Derivative
PI	Proportional Integral
PMSM	Permanent Magnet Synchronous Motor

LIST OF SYMBOL

r_a =	Line resistance of the winding,
L_a =	Equivalent line inductance of the winding
B_V=	Viscous friction coefficient
k_e =	Line back-EMF constant, expressed as, $\boldsymbol{k_e}$
T_L =	Load torque;
J =	Rotor moment of inertia;
R_X =	Phase resistance
T_e =	Electromagnetic torque
T_L =	Load torque
B_m =	Maximum value of Permant magnet density distribution in air gap;
ψ_m=	Maximum value of PM flux linkage of each winding
$f_A(\theta)$	back-EMF waveform function of phase A.

CHAPTER ONE

INTRODUCTION

1.1 Background of the study

Permanent Magnet Brushless DC (BLDC) motors is the most used industrial applications such as robotics, aerospace, and home appliances due to their high efficiency, compact size, and low maintenance requirements. However, achieving precise speed control of BLDC motors remains challenging because of nonlinearities, parameter variations, load disturbances, and external environmental factors affecting motor performance. Traditional PID controllers are widely applied in motor control systems because of their simple structure and ease of implementation. However, their performance can be limited when the system operates under changing conditions. In the presence of parameter uncertainties and dynamic disturbances, conventional PID controllers may experience problems such as overshoot, steady-state error, and reduced control performance. [1]

Advantage of permanent magnet BLDC Dc motor High efficiency, High power density ,Low maintenance requirements due to the absence of brushes , High reliability and long operational life , Fast dynamic response and low acoustic noise and reduced electromagnetic interferenc**e**

Brushless DC (BLDC) motors are widely utilized in many applications, including electric vehicles, robotics, HVAC systems, consumer electronics, computer equipment, semiconductor manufacturing, CD-ROM drives, medical devices, CNC machine feed drives, and extruder drive systems. In these applications, BLDC motors often operate under varying load conditions and are frequently subjected to different types of load disturbances. Such disturbances can significantly affect the motor's performance. Traditional control techniques are often unable to provide the desired speed regulation and accurate tracking performance while maintaining stability, especially when load disturbances and parameter variations are present**...**[2]

A control system is designed to regulate and manage the dynamic behavior of a plant or process, such as a BLDC motor, in order to achieve the desired performance. Among the various control techniques, adaptive control has gained significant attention due to its ability to handle system uncertainties and

parameter variations while maintaining good performance and accuracy. One of the widely used adaptive control approaches is Model Reference Adaptive Control (MRAC). MRAC is a direct adaptive control strategy in which the controller contains adjustable parameters along with an adaptation mechanism. This mechanism continuously updates the controller parameters so that the motor speed follows the desired reference model..The speed control for Permanent Magnet Brushless DC (BLDC) motors using Model Reference Adaptive Control (MRAC), Lyapunov-based stability analysis ensures that the motor speed converges to the desired reference speed despite disturbances and model uncertainties.

Specifically, this analysis guarantees that the speed tracking error (the difference between the actual motor speed and the reference speed) asymptotically approaches zero, meaning precise and stable speed regulation is achieved.

By applying Lyapunov theory in your MRAC design, you mathematically prove that the adaptive control parameters adjust themselves in a way that maintains the stability of the speed control system. This results in robust performance where the motor speed quickly adapts and settles at the commanded speed, even when subjected to varying loads or parameter changes. Thus, Lyapunov-based stability is critical for confirming that your adaptive MRAC speed controller can robustly and reliably regulate BLDC motor speed under all expected operating conditions. The MRAC controller adapts the control parameters in real-time to maintain robust and precise speed regulation under varying load and system dynamics, ensuring system stability and convergence through Lyapunov-based analysis.[3]

1.2 Statement of the problem

Permanent Magnet Brushless DC (BLDC) motors are widely used in industrial drives, robotics, and renewable energy systems due to their high efficiency, compact size, and maintenance-free operation enabled by electronic commutation. The performance of BLDC motors is significantly affected by: - Load disturbances ,Parameter variations (resistance, inductance, torque constant) ,Nonlinear back-EMF characteristics ,Temperature changes and Uncertainties during real-time operation and and supply voltage fluctuations

Base on Literature review such Traditional fixed-gain PI/PID controllers, commonly used in industry, are tuned only for nominal conditions and show severe to the large overshoot, the increased settling time based , steady-state error, and weak disturbance rejection capability in the control system

Although advanced methods such as fuzzy logic and sliding mode control have been investigated. While fuzzy, GA/PSO-tuned, or SMC variants demand complex tuning, suffer computational overhead, or introduce chattering. They often involve high computational complexity, chattering, or lack guaranteed stability. Therefore, there is a strong need for a simple, adaptive, and theoretically proven control strategy that can automatically adjust its parameters in real time to maintain excellent speed tracking and robustness. This thesis to apply a Model Reference Adaptive Control (MRAC) scheme using a modified MIT rule and Lyapunov-based adaptation mechanism to address these to achieve fast, accurate, and robust speed control of BLDC motors .

1.3 Objectives of the thesis

1.3.1 General objectives

The main objective of this thesis is to design a speed control system for a Permanent Magnet Brushless DC (BLDC) motor using a Model Reference Adaptive Control (MRAC).

1.3.2 Specific objective

- To analyze model stability of a Permanent Magnet BLDC
- To Design the MIT rule and Lyapunov stability method with MRAC model reference adaptive control
- To simulate and analyze the performance of the MRAC with gradient method (MIT rule) and Lyapunov stability method.
- To compare the performance of the MRAC with Lyapunov stability method a conventional PID controller.
- To analysis system stability using Lyapunov stability Method.

1.4 Scope of the study

The scope of this thesis is to design and simulation modal Reference Adaptive control (MRAC) with Lyapunov stability and MIT rul for Speed Control permanent Magnet Brushless Dc Motor only using MATLAB/Simulink by changing different Load Torque .

1.5 Significance of the Study

This thesis study was significant for Enhances motor performance to provides an advanced control method that improves speed accuracy, dynamic response, robustness of BLDC motor and Adaptive capability of the MRAC controller automatically adjusts its parameters in real time, Improved stability the application of Lyapunov theory ensures stable adaptation laws and guarantees global system stability.

1.6 Limitation of the study

This thesis study is conducted fully in MATLAB/Simulink; real hardware implementation is not included and Only speed control is addressed; torque ripple and position control are not covered.

CHAPTER TWO

LITERATURE REVIEW

2.1. Related work of Literature review

This chapter presents a review of the literature related to the topic of this thesis. Different control techniques used for parameter regulation and their reported system performance are discussed. In addition, the results obtained in previous studies are analyzed and compared. The differences between those works and the approach proposed in this thesis are also clearly explained.

Hutama , et al .(2018) [4] presented on the robust Adaptive Sliding Mode Control Design with GA for Brushless DC Motor. The gaps of the paper the study was designed to address several limitations found in prior research and conventional controllor schemes for Brushless DC Motor (BLDCM) speed control and the study identifies that existing control methods of the paper proposes its hybrid control method as a solution to address these limitations, aiming to improve system performance and accommodate for changes in working circumstances by incorporating fuzzy logic into the management of the converter DC bus voltage. The paper introduces and studies a unique hybrid control method for speed management of a Brushless DC (BLDC) motor. The use of advanced control with sliding control it is complex the variation of speed the motor.

M. GIRIBABU(2023) **[5]** presented the Brushless DC motor speed regulation with a fuzzy PID controller. The paper develops and studies a metaheuristic approach based on a tweaked version of the Harmony Search (HS) algorithm to find the optimal settings. The research focuses heavily on the optimization of the complex FOPID controller settings, which involves five adjustable parameters (Kp , Ki ,Kd, λ,μ). The relates to the limitations of control methods developed using simplified linear models when applied to the complex, real-world operation of the Brushless DC (BLDC) motor

Suwandi Dwi Sahputro et al. **(2017)[6]** presented that design and implementation of an adaptive PID controller for controlling the speed of a DC motor. The DC motors are favored for their ease of speed and position control, commonly using PID controllers for effective speed matching. A major challenge is that optimal PID constants (Kp, Ki, Kd) vary with motor characteristics, which can change over time.

Traditional methods for determining these values are often time-consuming. While adaptive control methods, such as minimum variance estimation and neural networks, have been explored, a significant gap remains: the need for a robust system that can not only set initial PID constants but also adaptively modify them online as motor parameters change. The authors propose an adaptive PID control strategy that calculates and tunes parameters online. This approach employs Recursive Least Squares (RLS) for parameter estimation and an online pole placement method to adjust PID constants, ensuring consistent motor performance despite variations.

Muhammed A. Ibrahim et al. (2019)[7] presented on that designing an optimal controller for Brushless DC (BLDC) motor speed control using a genetic algorithm (GA). While BLDC motors are favored in industrial applications for their efficiency and torque, precise speed and torque control is crucial, especially in sensitive settings. Traditional PID tuning methods, such as trial and error and MATLAB tuner applications, often lack reliability and accuracy for real-time responses, revealing a performance gap in high-performance control systems. To address this, the article proposes using GA to optimize PID parameters, minimizing Integral Absolute Error (IAE) and Integral Squared Error (ISE). Simulation results show that the GA-PID controller, particularly with the ISE objective function, significantly outperforms conventional tuning methods in rise time, settling time, and percentage overshoot.

H Q Yin, (2020) [8] presented that of the fuzzy adaptive PID control of brushless DC motor focuses designing a fuzzy adaptive PID control algorithm for brushless DC motors (BLDCMs). Research Gap Traditional PID controllers struggle with the complexities of BLDCMs, leading to poor adaptability and control. This study addresses these limitations by proposing a fuzzy adaptive PID method to enhance performance, robustness, and anti-interference capabilities. The paper did not consider variations in other parameters and utilized a basic fuzzy adaptive PID control method controller.

Ramya M.A. (2020) [9] presented that Design and Implementation of Particle Swarm Optimization (PSO) Tuned PID Controller for the Speed Control of Permanent Magnet Brushless DC motor (PMBLDC) . It focuses Developing a PID controller for PMBLDC motor speed control using Particle Swarm Optimization (PSO) for parameter tuning. Research Gap The study highlights the challenges of

effectively controlling PMBLDC motors, which are nonlinear and sensitive to parameter variations. While PID controllers are favored for their simplicity, their performance is heavily dependent on tuning methods. Limitations of Traditional Methods the Ziegler-Nichols method is time-consuming and often results in excessive overshoot and longer settling times..

Thang Nguyen Trong, (2017)[10] presented that Control to the for DC Motor based on the flatness Control. The gaps of the paper addresses limitations in controlling Direct Current (DC) motors, which remain widely used in industry. While PID controllers are popular, they struggle in high nonlinearity conditions, compromising control quality. Existing nonlinear control methods, such as input-output linearization, sliding mode control, and back stepping, have drawbacks like chattering phenomena and challenges in selecting appropriate Lyapunov functions. The paper proposes a flatness-based control system to enhance control quality for DC motors. However, flatness controllers perform best when motor parameters are known precisely, which is rarely the case in practice. This lack of accurate parameter knowledge leads to a static error between the desired and actual speeds when using flatness control alone.

Maycon Chimini Bosco **,** (2017) [11]**,** proposed that Estimation of Parameters and Tuning of a Speed PI of Permanent Magnet DC Motor Using Differential Evolution. The gap the study identifies several critical gaps in the control of small DC motors used in automated production processes Lack of Parameter Data, Design Challenges and Empirical Techniques

The paper highlights that the unknown parameters of permanent magnet DC motors hinder effective controller design, resulting in time-consuming empirical approaches and poorly selected parameters. To address these issues, the research focuses on developing methods for parameter estimation and controller tuning. It proposes a system that estimates motor parameters and optimally tunes a PI controller using a Differential Evolution algorithm. The study notes that errors from the estimation phase can affect the subsequent tuning process, presenting an additional challenge in achieving accurate control**.**

Heri Suryoatmojo (2020) [12] presented that Robust speed control of brushless dc motor based on adaptive neuron fuzzy inference system for electric motorcycle application. The gap is the paper

addresses the challenge of controlling Brushless Direct Current (BLDC) motors, commonly used in electric motorcycles for their high efficiency and reliability. While Proportional-Integral-Derivative (PID) controllers are popular due to their simplicity, they struggle with the complex and nonlinear nature of BLDC motors. Sudden changes in set-point and parameter variations worsen PID performance, as they are designed for linear systems. Thus, the article gap lies in the limitations of both traditional PID and Fuzzy-PID controllers in providing robust and adaptive speed control for BLDC motors, especially under sudden changes or parameter variations. The paper proposes the Adaptive Neuron Fuzzy Inference System (ANFIS) controller to address these shortcomings.

K. Harshavardhana Reddy ,(2017)[13] proposed that Hybrid adaptive neuron fuzzy based speed controller for brushless DC motor. The paper examines the critical topic of speed control in Brushless DC (BLDC) motors, which are widely utilized in various applications. While conventional controllers like the Proportional Integral (PI), Proportional derivative (PD) and the Proportional Integral-Derivative (PID) are favored for their simplicity and robustness, they exhibit certain disadvantages, including, larger rise times and settling times and Increased oscillations in steady state. The core article gap identified is the absence of controllers that can consistently deliver desired performance characteristics such as quick settling times, zero peak overshoot, and zero steady-state error when controlling BLDC motors across different operating conditions. To address these limitations, the paper proposes a hybrid adaptive neuron-fuzzy control technique.

Pranoti K. Khanke , (2016)[14] Presented on that Comparative Analysis of Speed Control of BLDC Motor Using PI, Simple FLC, and Fuzzy-PI Control . The gaps the paper addresses the need for efficient variable speed control, long-term stability, and good transient performance in Brushless DC (BLDC) motors, which are inherently nonlinear. Achieving optimal performance requires improved controllers that can adapt to these nonlinear conditions. The paper identifies specific limitations in existing control methods for BLDC motors. Conventional PI Controllers: While widely used, they perform poorly under various operating conditions, resulting in high peak overshoot, larger rise and settling times, and increased oscillations. They are ineffective in dynamic environments. The Simple Fuzzy Logic Controllers (FLC): Although they offer better performance than PI controllers, they require automatic

tuning and consume more time and memory in real-time applications. Despite improvements, their overshoot remains relatively high.

Prakash Salawria in (2017) [15] Presented on hat Implementation of PSO-Based Optimum Controller for Speed Control of BLDC Motor. The gap this paper addresses the speed control of Brushless Direct Current (BLDC) motors, which are widely used in industrial and vehicle applications due to their long operational life, high efficiency, dynamic response, and favorable speed-versus-torque characteristics. Additionally, their brushless design makes them less noisy. However, the study identifies significant challenges in controlling BLDC motors due to their coupling and nonlinear performance. Traditional control algorithms often struggle with poor precision and inadequate speed tracking, highlighting a gap in their effectiveness in managing these complexities. To tackle these issues, the paper proposes the use of an enhanced Particle. Swarm Optimization (PSO) algorithm for tuning the parameters of a PID controller in the BLDC motor servo system. The PSO technique aims to enable the PID controller to self-tune continuously in an online procedure, seeking the optimal set of parameters.

N.Arjuna Rao, et al.(2019),[16] presented on Speed Control of Brushless Dc Motor by Using PID and Fuzzy Logic Controller .the gaps of the paper PID control is widely used due to its simple structure and robust performance, but it is difficult to properly tune the gains when dealing with high order, time delay, and non-linear characteristics. It is often difficult to find optimal or near-optimal PID parameters using Z-N and T-L formulas in many industrial plants. Furthermore, the Z-N and T-L methods are time-consuming and force the system to the margin of instability. The traditional PID controller provides only a moderate response and performance compared to the fuzzy controller. To focus that The study evaluates the performance of a BLDC motor using conventional PID control and fuzzy logic control methods. Specifically, it implements and compares four PID tuning methods: Ziegler-Nicholas (Z-N), Tyreus-Luyben (T-L), Particle Swarm Optimization (PSO), and Fuzzy Logic Controllers in MATLAB/SIMULINK software. The overall conclusion is that PSO technique provides a better dynamic response than T-L and Z-N methods, and the Fuzzy controller yields a good and more stable performance than PID.

Fahrizal Auliansyah, et al. (2020) [17] presented on the Controlling Speed Of Brushless DC Motor By Using Fuzzy Logic Controller. the gaps of the paper The primary problem addressed is keeping

BLDC motor speed stable, responsive, and adaptive. Conventional control is not recommended for nonlinear conditions and load changes. Conventional control is also less effective applied to BLDC motors because it relies heavily on a mathematical model. A specific weakness of the Fuzzy Logic Controller is the difficulty of designing the system response in accordance with the desired results. Focus he paper discusses controlling BLDC motor speed by implementing a fuzzy logic controller (FLC). The FLC uses two inputs (error and delta error) to generate a PWM value to control the 3-phase inverter. The goal is to design a control system that is stable, responsive, and adaptive to control motor speed

Mekha M.L, et al. (2016), [18] presented on the Speed Control of BLDC Motors Using MRAC. The gaps of the paper when the plant parameter changes with respect to time, the constant gain PI controller action is not effective. Conventional PI controllers pose difficulties where there is control complexity such as nonlinearity, load disturbances and parametric variations. Since the Permagnet magnet brushless Dc motor has a nonlinear model of the linear proportional integral may no longer be suitable. To focus the research proposed a speed estimation algorithm based on Model Reference Adaptive Control (MRAC) to correct speed error. The MRAC based design determines adjustable PI gain parameters by referring to a reference model. The designed MRAPIC (Model Reference Adaptive PI Controller) scheme aims to faithfully adjust controller parameters corresponding to changes in plant parameters.

Md Mahmud, (2020) , [19] presented on the Modeling and Performance Analysis of an Adaptive PID Speed Controller for the BLDC Motor the gaps of the paper The driving circuit for BLDC motors can be costly and complex. Traditional controllers like PID require the implementation of adaptability for better performance.it focus Proposes a combined method using PID and a PID auto tuner, named the Adaptive PID controller (APIDC), to improve system adaptability. Simulation results showed the Adaptive PID controller achieved very low overshoot (0.197%) and a fast settling time (0.05 seconds) compared to other existing controllers like the FPA speed controller.

Dr. NAGESWARA RAO K ,et al. **[20]** presented on the speed control of BLDC motor using adaptive fuzzy pid controller (Project Report) the gaps of the paper Conventional PID controllers are difficult to tune parameters to achieve satisfactory control characteristics. Fuzzy PID controllers only use a single

set of rules for parameters like Kp, Ki, and Kd. It focus Proposes an improved Adaptive Fuzzy PID controller for BLDC motor speed control. The controller achieves better control performance, particularly demonstrating superiority over both Fuzzy PID and conventional PID controllers.

P. S. Vikhe , et al .(2020) , [21] presented on the Speed Control of BLDC Motor using Open Loop, PID Controller and Neural Network the gaps of the paper Conventional PID controllers are difficult to meet the execution requirements of BLDC motor.it focus Proposes a control technique based on the RBF neural system PID. The analysis shows that the proposed controller provides better performance compared to the traditional PID controller.

Rizqi Andry Ardiansyah, et al .(2018) , [22] presented on the Rotational Speed Control of Brushless DC Motor Using Genetic Algorithm Optimized PD Controller . The gaps of the Optimizing the gains of the PD controller is an essential task. The Conventional Ziegler- Nichols(ZN) tuning in overshoot(e.g., 6.67 under changeless step function) and high control action**.** To focus Proposes a Genetic Algorithm (GA) Optimized Proportional-Derivative (GA-PD) controller for rotational speed control of BLDC motor. The GA-PD achieved zero overshoot under constant step functions, offering better performance than the ZN-PD controller.

Fatih Adıgüzel, (2022) , [23] presented on the A periodic adaptive controller for the torque loop of variable speed brushless DC motor drives with non-ideal back-electromotive force. The gaps of the paper Output torque ripples are caused by parametric and periodically varying uncertainties, particularly non-ideal phase-to-phase back-EMF, which is often unknown or not precisely measurable in practical applications. It focus that Proposes a periodic adaptive controller for the torque loop of variable speed BLDC motor drives to minimize output torque ripples. It uses hybrid differential-periodic adaptation rules to estimate the unknown periodic signal (non-ideal back-EMF) and accounts for commutation switching.

H. Abdelfattah, (2021), [24] presented on the Adaptive Neuro-Fuzzy Technique for Speed Control of Six-Step Brushless DC Motor. The gap of the paper Previous research using ANFIS for speed control sometimes failed to offer profiles beyond speed (e.g., torque, current) or lacked comparison against other control methodologies. It focus Presents an Adaptive Neuro-Fuzzy Inference System (ANFIS)

controller for a Six-Step BLDC motor drive. The ANFIS controller aims to improve the motor speed profile, currents, and electromagnetic torque. It showed better performance (reduced overshoot and settling time) compared to classical PI and Fuzzy controllers.

Huang Jigang, (2019), [25] presented on the A Propertional– integralI controller optimized with modified differential evolution algorithm for speed control of BLDC motor. The gapes of the paper Conventional PID controllers are sensitive to system uncertainties in BLDC motors . It is difficult to adjust for the above precision and rapid speed dynamic performance. It focus that Proposes a PI control with modified Differential Evolution (DE) algorithm for speed control brushless dc motor . The uses an adaptive mutation factor and a multivariable fitness function to achieve better overshoot, settling time, and rising time results than conventional PI or PI with standard DE.

Manh-Cuong Nguyen, (2020). [26] The study focuses on the application of a Model Reference Adaptive Control (MRAC)–based adaptive control system for regulating the speed of a direct current (DC) motor. Previous research has shown that when the control system structure is simple, such as with conventional PID controllers, the control performance is often limited. On the other hand, achieving higher performance typically requires a more complex control structure or precise knowledge of the system parameters. To address this limitation, the study proposes an MRAC-based control approach for DC motors. This method aims to maintain a relatively simple control structure while improving the overall control performance and system response**.**. It can adapt to object transformation when parameters are unknown or changing. The system combines a traditional PID controller with an adaptive controller to adjust output to follow a reference model. . However, in this thesis, particular attention is given to the selection of an appropriate reference model and the analysis of load disturbances affecting the system. In addition, the performance of the modified MIT rule and the Lyapunov theory based Model Reference Adaptive Control (MRAC) approach is evaluated under different operating conditions. The objective is to demonstrate the effectiveness and robustness of the proposed adaptive control method in regulating the speed of the motor.

In general, the control techniques that to enhance the performance and efficiency of speed control in Brushless DC (BLDC) motors. These methods are designed to handle variations in operating conditions while maintaining reliable controller performance. When designing an effective controller, it is

important to consider different operating scenarios such as no-load conditions, varying load torque, and possible output disturbance signals. Taking these factors into account helps ensure that the controller can maintain stable and accurate performance under uncertain and changing conditions.

2.2 Summary of Literature Review

Above relative literature review speed control methods for Brushless DC (BLDC) motors. Traditional PID controllers face challenges with parameter variations and sudden load changes. Fuzzy PID controllers offer some improvements but still struggle with complex motor dynamics. Genetic Algorithms (GA) are proposed for optimizing PID parameters, showing significant performance enhancements. Adaptive control techniques are highlighted for their ability to adjust PID parameters online. Particle Swarm Optimization (PSO) is suggested as an effective tuning method. Hybrid approaches, combining fuzzy logic and neuron-fuzzy systems, improve control in non-linear environments. Common challenges include excessive overshoot and long settling times. The review emphasizes the need for robust tuning methods. Overall, a shift towards adaptive and efficient algorithms is essential for modern applications. In general While PID and its variants (fuzzy, GA/PSO-tuned, neuron-fuzzy) are widely used the main disadvantages identified in the above literature such as poor adaptability to parameter changes, difficulty handling nonlinearity, high overshoot, longer settling times, and the need for frequent retuning can basically be solved by using Model Reference Adaptive Control (MRAC). MRAC is the most important controller for advanced , and adaptive speed control of Brushless DC motors.

CHAPTER THREE

METHODOLOGY

3.1 Chapter overview

This chapter delves into the materials and methodologies employed in this thesis, include the Material , Methodology with the the mathematic modeling of permanent magnet brushless DC Motor , Basic Structure of Permanent Magnet Brushless DC (PMBLDC) Motors Additionally, a schematic diagram for the permant magent Brushless Dc motor.

3.2 Material

The software tools used in this thesis include Microsoft Office 2016, MATLAB (2020b), draw.io and Mendeley Desktop 1.19.8. MATLAB incorporating Simulink and various technical toolboxes serves as the primary computational platform. Microsoft Office 2016 is used for preparing and editing the thesis manuscript. Draw.io is employed for creating block diagrams and flowcharts, while Mendeley Desktop 1.19.8 facilitates citation management throughout the thesis. Additionally, Mathpix snipping tool 03.00.08 is used to generate mathematical equations and expressions in both Microsoft Word and PowerPoint.

3.3 Methodology

To successfully accomplish the objectives of this thesis, a structured sequence of methodological steps is followed. The first step involves identifying and clearly defining the research problem through comprehensive analysis. The second step addresses the research background, which is essential for understanding and modeling the performance characteristics of the permanent magnet brushless DC motor, particularly its nonlinear behavior. In the third phase, design a Model Reference Adaptive Control (MRAC), using modified MIT rule and Lyapunov stability based the speed control of the PMBLDC motor. The fourth phase evaluates the performance of the proposed control algorithm using MATLAB/Simulink. Finally, the thesis concludes with of results conculsion and recommendations for the future research endeavors. The methodology to be followed to illustrated the flow chart presented in figure 3.1

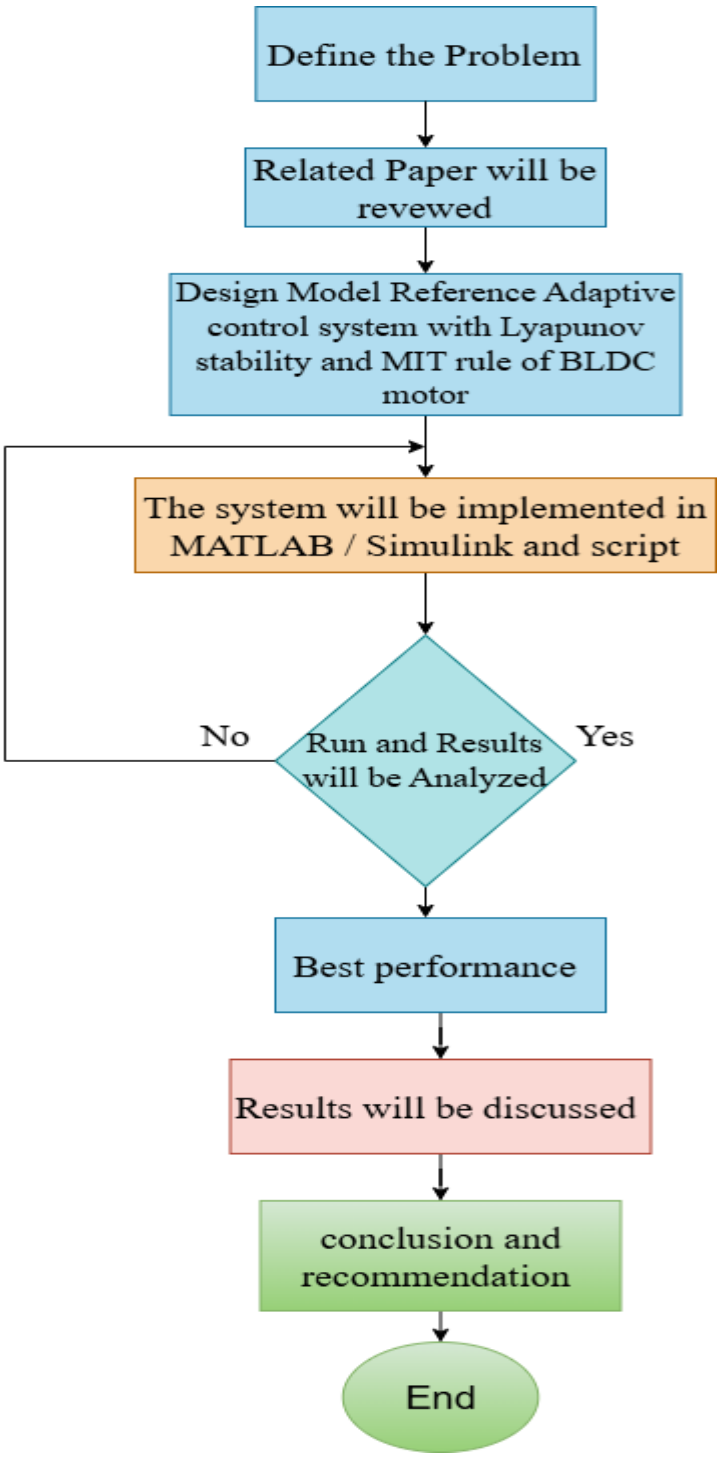


Figure 3.1 Thesis flow chart

3.4 Mathematic Modeling of permanent magnet brushless DC Motor

A clear mathematical model of a Brushless DC (BLDC) motor is essential for accurately analyzing its performance and designing effective control strategies. When developing such a model, it is important to take in to the motor's structural features and its operating principles. In general, a BLDC motor is composed of three main components: the motor itself, the power electronic drive, and the rotor position sensing mechanism. Because BLDC motors are available in different structural and can operate under various driving schemes, these aspects must be carefully considered during modeling.

This chapter begins by reviewing the commonly used BLDC motor structures and driving methods. Next, the most widely adopted mathematical representations are presented, the modeling of the BLDC motor is presented using several approaches **.**Th**e** Special attention is given to the behavior of phase currents and electromagnetic torque during the commutation process, as these factors have a significant impact on overall motor performance..[27][28]

3.5 Basic Structure of Permanent Magnet Brushless DC (PMBLDC) Motors

The fundamental principle behind the design of a Brushless DC motor is the replacement of the mechanical commutator with an electronic switching system. In conventional DC motors, brushes perform the commutation process, ensuring that the armature magnetic field remains perpendicular to the main magnetic field throughout operation. By eliminating brushes and using electronic commutation, BLDC motors reduce friction, minimize maintenance requirements, and improve overall efficiency and reliability**.**. However, this mechanical arrangement leads to wear, sparking, and frequent maintenance. To overcome these limitations, the "inverted DC motor" configuration was introduced, where the armature windings are located on the stator and the permanent magnets are mounted on the rotor. This design enables contactless commutation and significantly enhances the reliability of the motor.

Precise control of the motor's speed and direction is achieved by integrating to the passion sensor , a control unit, and a power electronic inverter within the BLDC motor system. These components operate

together to generate the appropriate switching signals based on rotor position, ensuring smooth and stable motor performance.

Compared with other types of electric motors, BLDC motors are commonly excited using square-wave currents, which provide several important benefits. These include efficient utilization of permanent magnets, a compact and lightweight structure, higher torque capability, and improved efficiency and operational reliability. Consequently, BLDC motors play a key role in improving product performance, extending service life, and reducing energy consumption. [27] These advantages have become even more pronounced with the development of high-performance and cost-effective NdFeB permanent magnet materials. As a result, BLDC motors are increasingly attractive for a wide range of industrial and commercial applications.

Numerous studies related to this thesis that have the focused on the speed control of permanent magnet BLDC motors in order to better understand their dynamic characteristics.

Structurally, a Brushless DC (BLDC) motor is composed of a stator that contains the armature windings and a rotor that is fitted with permanent magnets, making its configuration similar to that of a Permanent Magnet Synchronous Motor (PMSM). representation to the a cross-sectional of a four-pole brushless dc motor is shown in Figure 0.1, highlighting the arrangement of the stator and rotor component.

3.5 .1 The Cores of Stator

The stator of a BLDC motor shares a similar structure with that of conventional synchronous and induction motors, consisting of laminated iron cores and slots to accommodate the armature windings.. It consists of single-phase or multi-phase symmetrical windings embedded in a laminated iron core. These windings may be arranged in either a star (Y) or delta (Δ) configuration. However, considering both performance requirements and cost efficiency, the star connection is more widely used, in which the three-phase windings are symmetrically connected without a neutral terminal**.** Unlike traditional brushed DC motors, in which the armature windings are located on the rotor, BLDC motors place the armature windings on the stator. This arrangement improves heat dissipation and reduces thermal stress on the windings, leading to enhanced efficiency and longer motor lifespan.

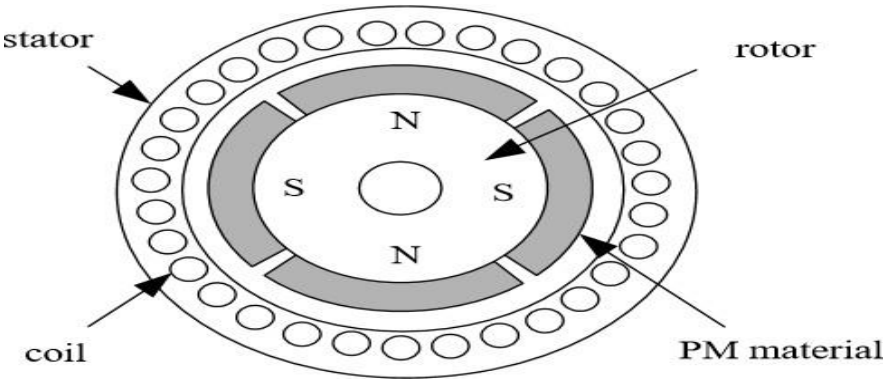


Figure 3.2: **Cross-sectional view of a Permanent Magnet Brushless DC (PMBLDC) motor,**

3.5.2 winding

Several winding configurations are commonly used in BLDC motors, including concentrated full-pitch windings, distributed full-pitch windings, and distributed short-pitch windings. The choice of winding type has a significant influence on the shape of the back electromotive force (back-EMF) and, consequently, on the overall motor performance.

In concentrated fully pitch windings, all conductors belonging to the same phase are placed within a single stator slot. As a result, the air gap of the flux density remains uniform for the phase. When the back-Electromotive force contributions from each conductor are combined, the resulting back-Electromotive force waveform closely follows the shape of the air gap fluxy density. In addition, the flat-top region of the back-Electromotive force wave form corresponds to the platform width of the air-gap flux density, allowing concentrated fully pitch of the windings to generate a back-Electromotvie force with a well to defined trapezoidal shape.

To enhance heat dissipation and make more efficient use of the stator's inner surface, the windings of a BLDC motor can be distributed evenly across multiple slots, creating what is referred to as a distributed winding. However, because of the spatial variation in the air-gap flux density, it is generally challenging to achieve an ideal square or trapezoidal back-EMF waveform with distributed windings. As an alternative, short-pitch windings can be employed, which reduce the length of the end

connections. This approach not only conserves copper material but also helps to minimize torque ripple and suppress harmonic components in the motor's output.

3.5.3 permanent Magnet Rotor

The rotor of a BLDC motor consists of permanent magnets arranged with a specific number of pole pairs, which may be mounted either on the surface of or embedded within the rotor's iron core. In modern BLDC motors, these permanent magnets are the commonly manufactured of the from rare-earth materials such as neodymium_iron_boron (NdFeB), due to their high coercively and strong magnetic energy density. In both BLDC and brushed DC motors, permanent magnets are used to establish the required magnetic field across the air gap. The key structural difference lies in their placement: in BLDC motors, the permanent magnets are installed on the rotor, whereas in brushed DC motors they are located on the stator.

Based on the arrangement of the permanent magnets, BLDC motor rotors can be classified into three typical structures:

1. **Surface-mounted permanent magnet rotor**: - In this configuration, radially magnetized, tile-shaped rare-earth permanent magnets are mounted directly on the surface of the rotor iron core. To reduce manufacturing cost, these tile-shaped magnets can also be formed by assembling rectangular magnet segments. During motor design, this structure is often preferred with a pole arc width greater than 120 electrical degrees, as it helps produce a near-square density and the reduces to torque ripple.
2. **The Magneted embedded rotor: -** In magnet-embedded rotors, rectangular permanent magnets are buried within the rotor iron core. This configuration enables better magnetic flux concentration, as the flux across a single pole pitch is produced by two adjacent poles working in parallel**.** To prevent unwanted magnetic coupling and leakage, magnetic isolation techniques or a stainless-steel shaft are typically employed in this type of rotor.

3 . **Magnetic Loop Rotor**- In the magnetic loop rotor configuration, a radially magnetized ring of rare-earth permanent magnets with multiple poles is mounted around the rotor iron core. This design is

commonly employed in low-power BLDC motors because of its simple construction, ease of manufacturing, and cost-effectiveness.

3.5.4 Position Sensor

Position sensors in a BLDC motor are used to detect the rotor's position and convert it into an electrical signal, which provides the necessary commutation information to the control circuitry. This allows the motor windings to be energized in the correct sequence based on the rotor's position, enabling continuous rotation of the permanent magnet rotor due to the stepping rotating magnetic field generated in the air gap. Various types of position sensors are available, each with distinct the characteristics. Of the Currently, electromagnetic(emf),in the photoelectric, and magnetic sensors are widely used in brushless dc motors. Among these, Hall-effect sensors a type of magnetic sensor are particularly popular because of their compact size, low cost, and ease of use.

3.6 Differential Equation Model

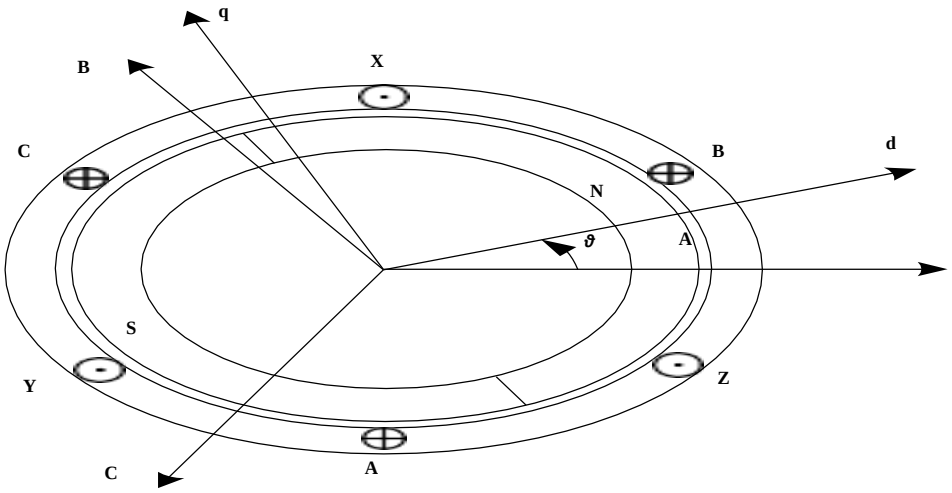
In this section, a mathematical model of a three-phase, two-pole BLDC motor is developed using differential equations. The stator is equipped with Y-connected, the full-pitch the windings, while the rotor has a non-salient pole design. To accurately detect rotor position and enable proper electronic commutation, three Hall-effect sensors are symmetrically placed around the stator, each separated by 120 electrical degrees. This configuration ensures that the motor windings are energized in the correct sequence, allowing smooth and continuous rotation of the rotor**..**[27]

To derive the differential equation model of the BLDC motor, the following simplifying assumptions are adopted:

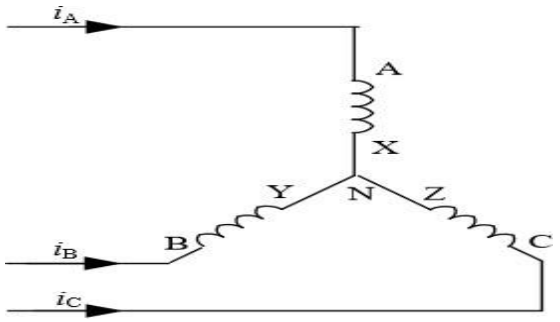
- Core saturation effects, as well as eddy current and hysteresis losses, are neglected.
- Armature reaction is ignored, and the air-gap magnetic field is assumed to have a trapezoidal distribution with a flat-top width of 120 electrical degrees.
- Cogging torque is neglected, and the conductors are considered to be continuously and uniformly distributed along the armature surface.

- The power switches and freewheeling diodes in the inverter are assumed to operate as ideal switching devices.

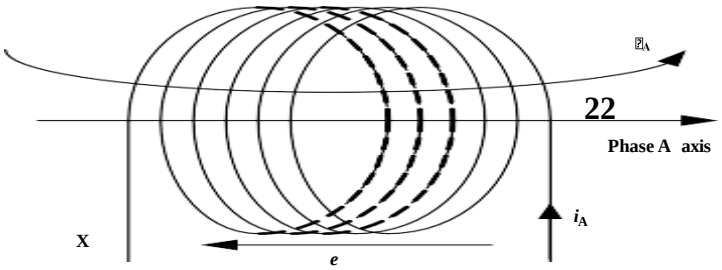
Based on these assumptions, a simplified equivalent schematic of the BLDC motor can be obtained, as illustrated in Figure 0.3.



(a) The Brusless DC motor structure



(b) The types of connection winding



(c) The positive direction Phase A

Figure 3.3 permanet Magnet breshless Dc motor Schematic diagram

With respect to the positive reference direction to indicated in Figure 0.3, the voltage of each stator phase comprising the resistive of the drop voltage and the electromotive force to induced can be to identify as follows:

$$\boldsymbol{u_x = R_x i_x + e_{\psi x}} \quad (3.1)$$

The following notations are used in the BLDC motor model:

$\boldsymbol{U_x}$= Phase voltage, where the subscript xxx represents phases A, B, or C.

$\boldsymbol{i_x}$ = phase current

$\boldsymbol{e_{\psi x}}$ = phase-induced Electromotive force

$\boldsymbol{R_x}$ = phase resistance.

For a three-phase symmetrical winding, all phase resistances are equal, and they satisfy the condition:

$$\boldsymbol{R_A = R_B = R_C = R}$$

The electromotive force (EMF) induced in the windings is proportional to the rate of change of the magnetic flux linkage. Considering that the positive directions of the induced EMF and the flux linkage, as defined in Figure 0.3, are opposite to the orientation given by the right-hand screw rule, the induced Electromotive force can be expressed as:

$$\boldsymbol{e_{\psi x} = \frac{d\psi_x}{dt}} \quad (3.2)$$

Taking phase, a for example, the flux is given as

$$\boldsymbol{\psi_A = L_A i_A + M_{AB} i_B + M_{AC} i_C + \psi_{pm}(\theta)} \quad (3.3)$$

Then

$\psi pm\ (\theta)$ = Permanent Magnet flux linkage of phase A;

θ = The rotor position of the the angle between rotor *d*-axis and the axis of phase A;

$\boldsymbol{L_A}$ = The self-inductance of phase A

$\boldsymbol{M_{AB}}$,$\boldsymbol{M_{AC}}$= mutual inductance of phase A , phase B and phase C.

The flux linkage $\psi pm\ (\theta)$ magnitude of depends on to the magnetic field distribution of the permanent magnets in the air gap. The radial component of the Permanet Magnet air-gap of the magnetic field exhibits a trapezoidal to distribution of the along the inner surface of the stator, as illustrated in Figure 0.4.

As illustrated in Figure 0.4, when the rotor rotates in the anticlockwise direction, the phase A (AX) winding effectively moves along the y-axis. As a result, the flux linkage of phase A changes with the rotor position. At a specific rotor position, denoted by θ=a flux produced by the permanent magnets and linked with phase A can be expressed as:

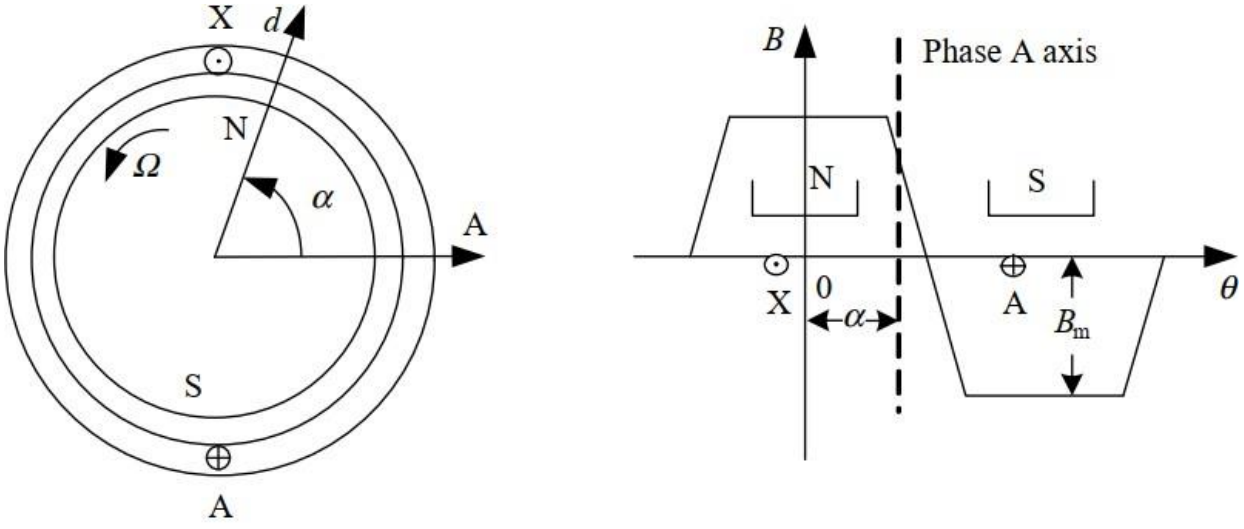
$$\boldsymbol{\psi_{pm}(\alpha) = N\phi_{pm}(\alpha)} \qquad (\mathbf{3.4})$$

$$\varphi_{\mathrm{pm}}(\alpha) = \int_{-\frac{\pi}{2}}^{\frac{\pi}{2}+\alpha} \beta(\theta) s d\theta \qquad (3.5)$$

Where

$\psi pm\ (\alpha)$ — Permeant Magnet flux

B($\boldsymbol{\theta}$) — The radial flux density of the permanent magnet rotor in the air gap follows a trapezoidal distribution along the y-axis



(a) Rotor position (b) Flux distribution

Figure 3.4: Permanent magnet flux linkage

- N – the number of turns of winding.
- S – Product of the rotor radius and the effective length of the conductors.

.

By substituting Equations (3.2)–(3.5) into Equation (3.1), the phase voltage of phase A can be expressed as:

$$\boldsymbol{u_A = Ri_A + \frac{d}{dt}\left(L_A i_A + M_{AB} i_B + M_{AC} i_C + \psi_{pm}\right)}$$

Expanding the flux linkage of the permanent magnets gives:

$$\boldsymbol{u_A} \quad = \boldsymbol{Ri_A + \frac{d}{dt}(L_A i_A + M_{AB} i_B + M_{Ac} i_C) + \frac{d}{dt}\left[NS \int_{\frac{\pi}{2}+\theta}^{\frac{\pi}{2}+\theta} (B(x)dx\right]}$$

Simplifying, the phase voltage can be written as:

$$u_A \quad = Ri_A + \frac{d}{dt}(L_A i_A + M_{AB} i_B + M_{AC} i_C) + e_A \qquad (3.6)$$

The $\boldsymbol{e_A}$ the electro motive force of phase A Equation (3.6). Both the self-inductance and the mutual inductance of the windings are proportional to $\boldsymbol{N^2}$, where N the number of turns, and are influenced .

In other words, the inductance values depend on the winding configuration and the magnetic path through which the flux flows, affecting the dynamic response of the motor.

$$\boldsymbol{L_A = N^2 \Lambda_A} \tag{3.7}$$

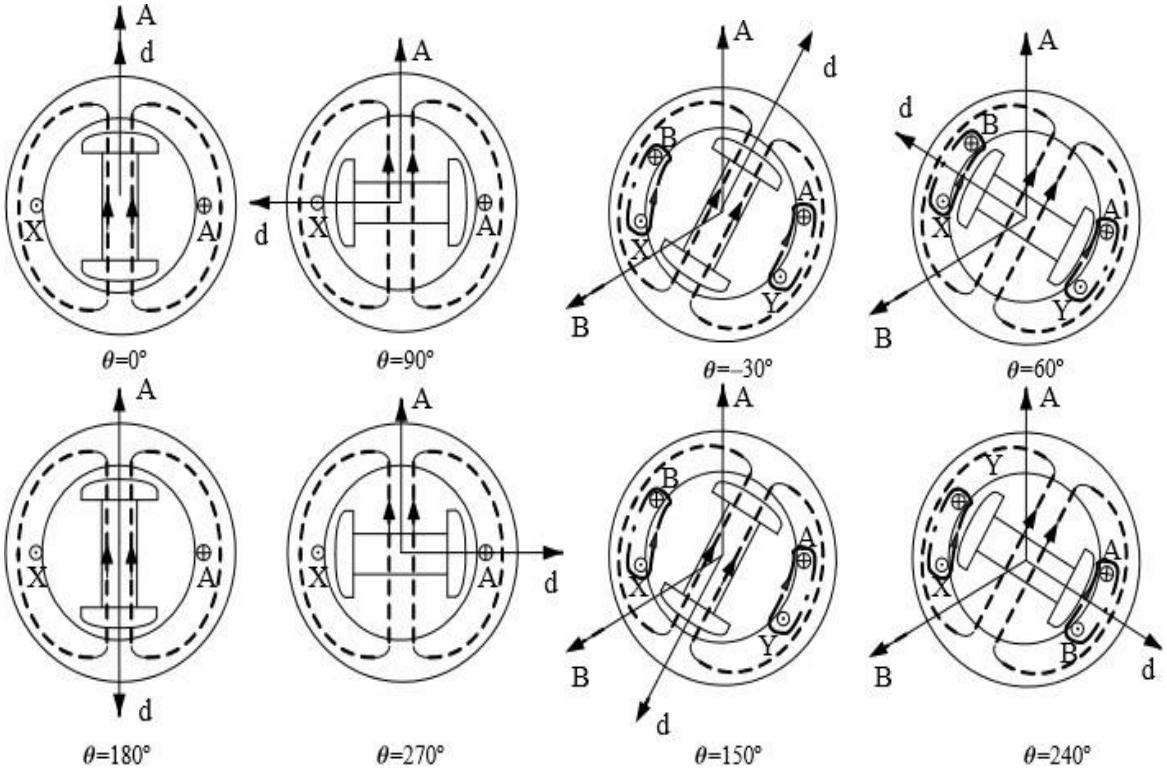
$$\boldsymbol{M_{AB} = N^2 \Lambda_{AB}} \tag{3.8}$$

Where

Δ_A = self-presence of phase A magnetic path

Δ_{AB} = mutual presence between phases A and B

In a salient-pole rotor, the magnetic permeability along the d-axis differs from that along the q-axis. Consequently, both the self-inductance and the mutual inductance of the windings vary depending on the rotor position.[29]



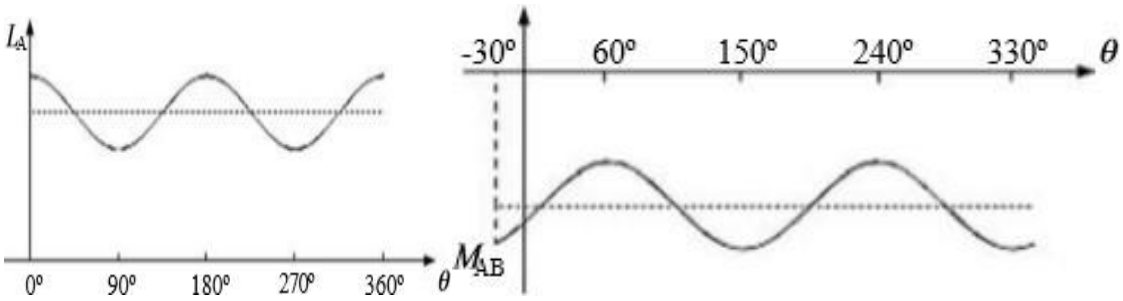


Figure 3.5 The Rotor the magnetic of circuit. [27]

In most BLDC motors, a surface-mounted, non-salient rotor is employed. Under this configuration, the winding inductances remain constant over time. Moreover, because the three-phase stator windings are symmetrical, the self-inductances of each phase are equal, and the mutual inductances between phases are also identical.

That is

$L_A = L_B = L_C = L, M_{AB} = M_{BA} = M_{BC} = M_{CB} = M_{AC} = M_{CA} = M$. Substituting them into Equation (3.6), We can get

$$\boldsymbol{u_A = Ri_A + L\frac{di_A}{dt} + M\frac{di_B}{dt} + M\frac{di_C}{dt} + e_A} \qquad (3.9)$$

In which :-

The back-Electromotive force of phase A can be derived from the rate of change of the flux linkage as follows:

$$\boldsymbol{e_A = \frac{d}{dt}\left[NS\right]_{-\frac{\pi}{2}+\theta}^{\frac{\pi}{2}+\theta} B(x)dx\Big] = NS\left[B\left(\frac{\pi}{2}+\theta\right) - B\left(-\frac{\pi}{2}+\theta\right)\right]\frac{d\theta}{dt}}$$

$$\boldsymbol{= NS\omega\left[B\left(\frac{\pi}{2}+\theta\right) - B\left(-\frac{\pi}{2}+\theta\right)\right]} \qquad (3.10)$$

Where ω is the electrical angular speed of the motor. Considering the distribution of the magnetic flux density in the air gap Figure 0.5 (b), and noting that B(θ) has a period of 2π and satisfiys B (θ + π) = –B(θ), Equation (3.10) simplifies to:

$$\boldsymbol{e_A = NS\omega[B(\frac{\pi}{2}+\theta) - B(-\frac{\pi}{2}+\theta)} \quad \boldsymbol{= NS\omega[B(\frac{\pi}{2}+\theta) - B\left(\frac{\pi}{2}+\theta+\pi-2\pi\right)}$$

$$\boldsymbol{e_A = 2NS\omega B(\frac{\pi}{2}+\theta)} \qquad (3.11)$$

Then, the θ -dependent back-EMF wave of phase A is $\frac{\pi}{2}$ ahead of the distribution of the magnetic density in air gap, and eA can be expressed as:-

$$e_A = 2NS\omega B_m f_A(\theta) = \omega\psi_m f_A(\theta) \qquad (3.12)$$

Where

B_m = Maximum value of the permanent magnet flux density in the air gap.

$\boldsymbol{\psi_m}$ = Maximum Permanet magnet flux linkage of each winding, given by $\boldsymbol{\psi_m}$ = 2NS$\boldsymbol{B_m}$

$\boldsymbol{f_A}(\theta)$ = back-Electromotive force waveform function of phase A.

It should be noted that $\boldsymbol{f_A}(\theta)$ exhibits a trapezoidal distribution with respect to the rotor position, with maximum and minimum values of 1 and –1, respectively. The corresponding waveform, along with its phase relationship to B($\boldsymbol{\theta}$) and $\boldsymbol{e_A}$ is illustrated in Figure 0.7. For a three-phase symmetrical winding, the back-EMF functions for the other phases can be expressed as:

$$\boldsymbol{f_{B(\theta)} = f_{A\left(\theta+\frac{2\pi}{3}\right)}} \ , \qquad \boldsymbol{f_C(\theta) = f_{A\left(\theta+\frac{2\pi}{3}\right)}} \ .$$

From Equation (3.10), it can be seen that $\boldsymbol{e_A}$ represents a rotating back-Electromotive force produced by the winding flux linkage resulting from the rotor's rotation. Moreover, for a three-phase balanced system, the phase currents satisfy the relationship:-

Then the current of three phas apply

$$\boldsymbol{i_B + i_B + i_C = 0} \qquad (3.13)$$

This condition ensures that the sum of instantaneous phase currents in a star-connected BLDC motor is always zero, maintaining electrical neutrality and balanced operation.

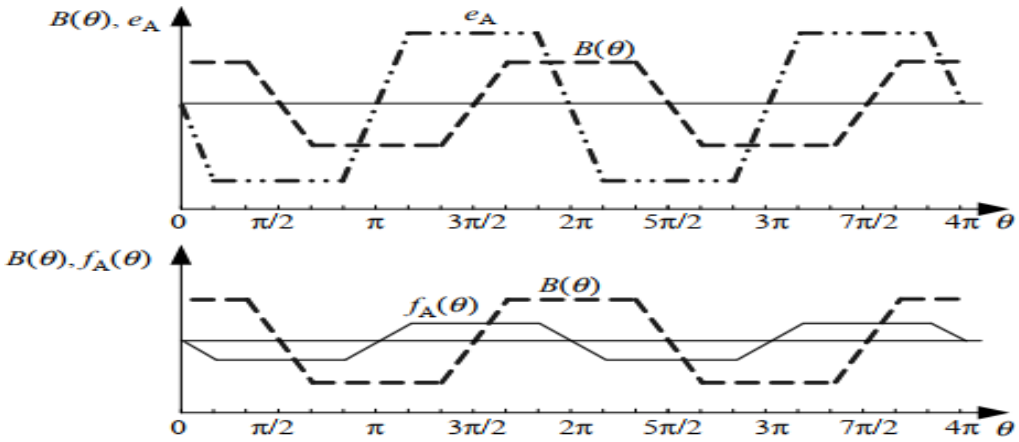


Figure 3.6 presents the phase same character B (**θ**), $\boldsymbol{fA}$ (**θ**) [27]

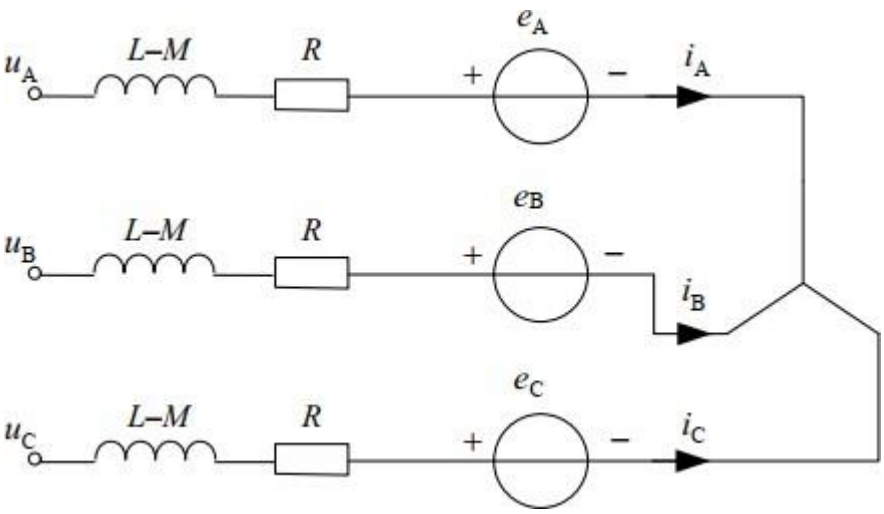


Figure 0.7 The same circuit Permanet Magnet Brushless Dc motor

Equation (3.9) can be further simplified as

$$\boldsymbol{u_A = Ri_A + (L - M)\frac{di_A}{dt} + e_A} \tag{3.14}$$

Then, the matrix form of phase voltage equation of BLDC motor can be expressed as

$$\begin{bmatrix} \boldsymbol{u_A} \\ \boldsymbol{u_B} \\ \boldsymbol{u_C} \end{bmatrix} = \begin{bmatrix} \boldsymbol{R} & \boldsymbol{0} & \boldsymbol{0} \\ \boldsymbol{0} & \boldsymbol{R} & \boldsymbol{0} \\ \boldsymbol{0} & \boldsymbol{0} & \boldsymbol{R} \end{bmatrix} \begin{bmatrix} \boldsymbol{i_A} \\ \boldsymbol{i_B} \\ \boldsymbol{i_C} \end{bmatrix} + \begin{bmatrix} \boldsymbol{L - M} & \boldsymbol{0} & \boldsymbol{0} \\ \boldsymbol{0} & \boldsymbol{L - M} & \boldsymbol{0} \\ \boldsymbol{0} & \boldsymbol{0} & \boldsymbol{L - M} \end{bmatrix} \frac{\mathbf{d}}{\mathbf{d}t} \begin{bmatrix} \boldsymbol{i_A} \\ \boldsymbol{i_B} \\ \boldsymbol{i_C} \end{bmatrix} + \begin{bmatrix} \boldsymbol{e_A} \\ \boldsymbol{e_B} \\ \boldsymbol{e_C} \end{bmatrix} \tag{3.15}$$

According to Equation (3.15), the equivalent circuit of the Brushless DC motor is illustrated in Figure 0.7

In most practical BLDC motor applications, the stator windings are connected in a Y (star) configuration without a neutral point, which makes direct measurement of the phase voltages challenging. Consequently, developing a mathematical model based solely on phase voltages may not always be practical. In contrast, the line voltages are easier to measure and, when the corresponding power transistors are conducting, are approximately equal to the DC bus voltage. For this reason, modeling the motor using line voltages is more suitable for practical implementation. The line voltage equations can be obtained by subtracting the respective phase voltage equations, as follows**:**

The line voltage equations can be derived by subtracting the corresponding phase voltage equations, as follows:

$$\begin{bmatrix} u_{AB} \\ u_{BC} \\ u_{CA} \end{bmatrix} = \begin{bmatrix} R & -R & 0 \\ 0 & R & -R \\ -R & 0 & R \end{bmatrix} \begin{bmatrix} i_A \\ i_B \\ i_C \end{bmatrix} + \begin{bmatrix} L-M & M-L \\ 0 & L-M \\ M-L & 0 \end{bmatrix} \frac{M-L}{L-M} \frac{d}{dt} \begin{bmatrix} i_A \\ i_B \\ i_C \end{bmatrix} + \begin{bmatrix} e_A - e_B \\ e_B - e_C \\ e_C - e_A \end{bmatrix} \quad \textbf{(3.16)}$$

Similar to conventional DC motors, the analysis of power and torque in a BLDC motor can be approached from the perspective of energy transfer. During operation, electrical power is drawn from the source; While a small portion of the input power is lost as copper and iron losses, the majority is transferred across the air gap to the rotor as electromagnetic torque. The power delivered to the rotor, commonly referred to as the electromagnetic power, can be calculated as the sum of the products of the phase currents and their corresponding back electromotive forces (back-EMFs) for all three phases.

That is

$$p_e = e_A\, i_A + e_B i_B \quad + e_C i_C \qquad (3.17)$$

Ignoring the mechanical loss and stray loss, the electromagnetic power is totally turned into kinetic energy, so

$$\boldsymbol{P_e = T_e \Omega} \quad (3.18)$$

Where

T_e = Electromagnetic torque;

Ω = Rotat of angular velocity

Hence, from Equations (3.17) and (3.18), we can get

$$\boldsymbol{T_e = \frac{e_A i_A + e_B i_B + e_C i_C}{\Omega}} \quad (3.19)$$

Substituting Equation (3.12) into Equation (3.19), another form of the torque equation can be represented as

$$\boldsymbol{T_e = p[\psi_m f_A(\theta) i_A + \psi_m f_B(\theta) i_B + \psi_m f_C(\theta) i_C]} \quad (3.20)$$

Here, p, represents the number of pole pairs.

When a BLDC motor operates in the 120° conduction mode, and the transient effects during commutation are neglected, only two of the three phase windings conduct current at any given time. These currents have equal magnitude but flow in opposite directions, while the third phase remains inactive in a Y-connected stator configuration. This conduction pattern ensures continuous torque production and contributes to the characteristic trapezoidal back-EMF operation of the motor**.**.[30]

It should be noted that the values of f(θ) in the flat-top region of the back-EMF are opposite for different phases. Consequently, Equation (2.20) can be further simplified as follows:

$$\boldsymbol{T_e = 2p\psi_m i_A = K_T i} \quad (3.21)$$

Where

$\boldsymbol{K_T}$ = The torque coefficient;

I = The steady phase current.

To develop a complete mathematical model of the electromechanical system, the mechanical motion equation must also be incorporated, expressed as follows:

$$\boldsymbol{T_e - T_L = J\frac{d\Omega}{dt} + B_v\Omega} \quad (3.22)$$

Where

$\boldsymbol{T_L}$ = Load torque;

J = Rotor moment of inertia;

$\boldsymbol{B_V}$ = Viscous friction coefficient.

Thus, Equations (3.15), (3.19) and (3.22) constitute the differential equation mathematical model of the BLDC motor.

3.6.1 Transfer Functions

The transfer function is a fundamental concept in control theory, and mathematical models based on transfer functions are widely used in automatic control applications. Many classical control design and analysis techniques, such as the root-locus method and frequency-response analysis, rely directly on the system's transfer function.

For BLDC motors, the transfer function is essential for both performance analysis and control system design. Unlike conventional brushed DC motors, the stator windings of a BLDC motor are energized based on the rotor position, and the motor typically has three or more phases. However, for any phase that is actively conducting, the processes of back-EMF generation and electromagnetic torque production are fundamentally the same as in a brushed DC motor. This similarity allows many of the same analytical techniques used for brushed DC motors to be applied to BLDC motor modeling and control.Assuming a three-phase BLDC motor is operated in two-phase conduction mode using a full-bridge drive, when the windings of phases A and B are conducting, the system can be described as follows:

$$\begin{cases} \boldsymbol{iA} = -\boldsymbol{i_B} = \boldsymbol{i} \\ \frac{\boldsymbol{diA}}{\boldsymbol{dt}} = -\frac{\mathbf{d}\boldsymbol{i_B}}{\mathbf{d}\boldsymbol{t}} = \frac{\mathbf{d}\boldsymbol{i}}{\mathbf{d}\boldsymbol{t}} \end{cases} \quad (3.23)$$

Thus, the line-voltage U_{AB} in Equation (3.16) can be rewritten as

$$\boldsymbol{u_{AB}} = \mathbf{2}\boldsymbol{Ri} + \mathbf{2}(\boldsymbol{L} - \boldsymbol{M})\frac{\mathbf{d}\boldsymbol{i}}{\mathbf{d}\boldsymbol{t}} + (\boldsymbol{e_A} - \boldsymbol{e_B}) \quad (3.24)$$

Neglect the transient effects during out of consideration (i.e. ignore the trapezoid bevel edge), then the steady $\boldsymbol{e_A}$ and $\boldsymbol{e_B}$ are equal in amplitude and opposite in direction when phases A and B are turned on. So, Equation (3.24) can be expressed as

$$\boldsymbol{u_{AB}} = \boldsymbol{U_d} = \mathbf{2}\boldsymbol{Ri} + \mathbf{2}(\boldsymbol{L} - \boldsymbol{M})\frac{\mathbf{d}\boldsymbol{i}}{\mathbf{d}\boldsymbol{t}} + \mathbf{2}\boldsymbol{e_A} = \boldsymbol{r_a i} + \boldsymbol{L_a}\frac{\mathbf{d}\boldsymbol{i}}{\mathbf{d}\boldsymbol{t}} + \boldsymbol{k_e}\boldsymbol{\Omega} \quad (3.25)$$

Where

$\boldsymbol{r_a}$ = Line resistance of the winding, where $\boldsymbol{r_a}$=2R;

$\boldsymbol{L_a}$ = Equivalent line inductance of the winding, given by , $\boldsymbol{L_a}$=2(L – M);

$\boldsymbol{k_e}$ = Line back-EMF constant, expressed as, $\boldsymbol{k_e}$ = 2pψm = 4pNS$\boldsymbol{B_m}$

Equation (3.25) represents the armature voltage loop equation for the case when two phase windings are conducting, and the corresponding equivalent circuit is illustrated in Figure 0.8. This formulation is essential for analyzing the electrical dynamics of the BLDC motor during operation in the 120°

conduction mode**.** It should be noted that the equivalent circuit depicted in Figure 0.8.

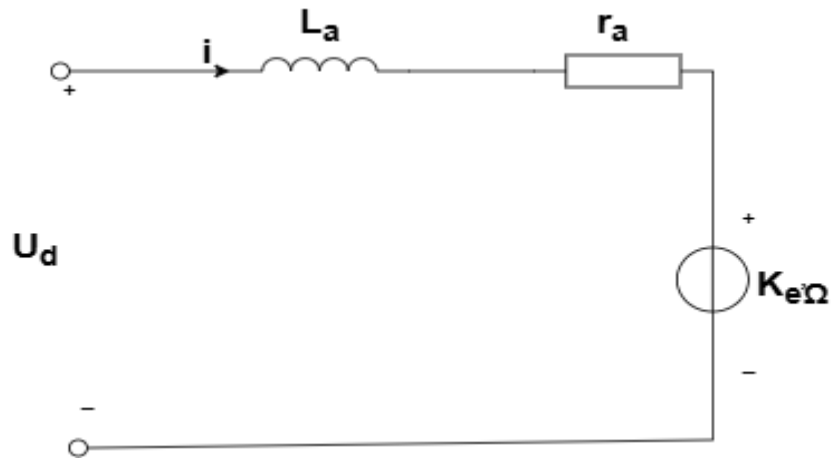


Figure 3.8: The equal circuit a brushless dc motor during operation

The In Equation (3.25), that the phase current to expressed as the function of the rotor's angular velocity to the transfer function of the motor can be derived by relating the DC bus voltage to the angular velocity . By adding Equation (3.21) to Equation (3.22), the same function is obtained::

$$\boldsymbol{K_{\mathrm{T}} i - T_{\mathrm{L}} = J\frac{\mathrm{d}\Omega}{\mathrm{d}t} + B_{\mathrm{v}}\Omega} \qquad (3.26)$$

First, when the BLDC motor runs with no load, the current is given as

$$\boldsymbol{i = \frac{J}{K_{\mathrm{T}}}\frac{\mathrm{d}\Omega}{\mathrm{d}t} + \frac{B_{\mathrm{v}}}{K_{\mathrm{T}}}\Omega} \qquad (3.27)$$

Substituting Equation (3.27) into Equation (3.25), we get

$$\boldsymbol{U_{\mathrm{d}} = r_{\mathrm{a}}\left(\frac{J}{K_{\mathrm{T}}}\frac{\mathrm{d}\Omega}{\mathrm{d}t} + \frac{B_{\mathrm{v}}}{K_{\mathrm{T}}}\Omega\right) + L_{\mathrm{a}}\frac{\mathrm{d}}{\mathrm{d}t}\left(\frac{J}{K_{\mathrm{T}}}\frac{\mathrm{d}\Omega}{\mathrm{d}t} + \frac{B_{\mathrm{v}}}{K_{\mathrm{T}}}\Omega\right) + k_{\mathrm{e}}\Omega} \qquad (3.28)$$

Also, it can be rearranged as

$$\boldsymbol{U_{\mathrm{d}} = \frac{L_{\mathrm{a}}J}{K_{\mathrm{T}}}\frac{\mathrm{d}^2\Omega}{\mathrm{d}t^2} + \frac{r_{\mathrm{a}}J + L_{\mathrm{a}}B_{\mathrm{v}}}{K_{\mathrm{T}}}\frac{\mathrm{d}\Omega}{\mathrm{d}t} + \frac{r_{\mathrm{a}}B_{\mathrm{v}} + k_{\mathrm{e}}K_{\mathrm{T}}}{K_{\mathrm{T}}}\Omega} \qquad (3.29)$$

By applying the Laplace transform to Equation (2.29), the transfer function of the BLDC motor can be expressed as follows:

$$\boldsymbol{G_{\mathrm{u}}(s) = \frac{\Omega(s)}{U_{\mathrm{d}}(s)} = \frac{K_{\mathrm{T}}}{L_{\mathrm{a}}Js^2 + (r_{\mathrm{a}}J + L_{\mathrm{a}}B_{\mathrm{v}})s + (r_{\mathrm{a}}B_{\mathrm{v}} + k_{\mathrm{e}}K_{\mathrm{T}})}} \qquad (3.30)$$

Therefore, the control system structure of a BLDC motor operating under no-load conditions can be

represented as shown in Figure 0.9.

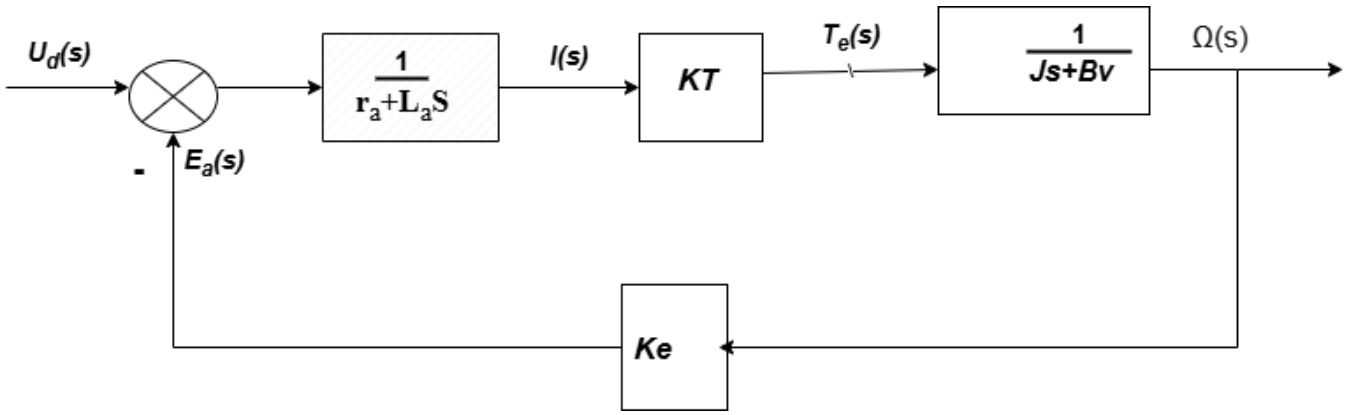


Figure 3.9: Configuration of a brushless dc motor operating under no-load conditions

Equation (3.30) indicates that the BLDC motor can be modeled as a second-order system, and therefore, it can be rearranged as follows:

$$\boldsymbol{G_u(s) = \frac{K_T}{r_a B_v + k_e K_T} \frac{\omega_n^2}{(s^2 + 2\xi\omega_n s + \omega_n^2)}} \qquad (3.31)$$

Where

$$\boldsymbol{\omega_n = \sqrt{\frac{r_a B_v + k_e K_T}{L_a J}}}$$

$$\boldsymbol{\xi = \frac{1}{2} \frac{r_a J + L_a B_v}{\sqrt{L_a J}\sqrt{(r_a B_v + k_e K_T)}}}$$

from Equation (2.31), it can be seen that the characteristic equation of the BLDC motor's second-order system has two roots, expressed as:

$$S_{1,2} = -\xi\,\omega_n \pm \omega_n \sqrt{\boldsymbol{\xi^2 - 1}}$$

The system's response time is determined by the natural frequency and the damping ratio . For a unit step input, the speed at which the response curve converges is primarily influenced by $\boldsymbol{\omega_n}$ a higher $\boldsymbol{\omega_n}$ generally results in faster convergence. Meanwhile, the damping ratio ζ dictates the nature of the system's eigenvalues and the overall shape of the response curve. Depending on its value, the system can be underdamped, critically damped, or overdamped, each exhibiting distinct dynamic behavior., $0< \xi <1$, $\xi=1$ and $\xi>1$.

Let the mechanical time constant be $\boldsymbol{t_m = \frac{r_a J + L_a B_v}{r_a B_v + k_e K_T}}$ and the electromagnetic time constant be $\boldsymbol{t_e = \frac{L_a J}{r_a J + L_a B_v}}$, then Equation (3.30) can be rewritten as

$$\boldsymbol{G_u(s) = \frac{K_T}{r_a B_v + k_e k_T} \frac{1}{(s^2 t_m t_e + s t_m + 1)}} \quad (3.32)$$

In general, the mechanical time constant of a BLDC motor is significantly larger than its electrical (electromagnetic) time constant, i.e., i.e. $t_m \gg t_e$, Therefore, the transfer function presented in Equation (3.32) can be further simplified as follows:

$$\boldsymbol{G_u(s) \approx \frac{K_T}{r_a B_v + k_e K_T} \frac{1}{(s^2 t_m t_e + s t_m + s t_e + 1)}} \quad (3.33)$$

$$\boldsymbol{= \frac{K_T}{r_a B_v + k_e K_T} \frac{1}{(s t_m + 1)(s t_e + 1)}}$$

From Equation (3.33), it can be observed that the transfer function of a Permanent Magnet BLDC motor can be represented as two inertia elements connected in series. Figure 0.10 shows the corresponding speed response of the system to a step input. **.** When a step voltage is applied to the motor, the current initially responds to the voltage variation according to the electrical dynamics represented by the $\boldsymbol{\frac{1}{(st1)}}$term, the electrical time constant. Subsequently, the motor speed responds to the change in current through another dynamic element represented by the $\boldsymbol{\frac{1}{(st1)}}$ where $\boldsymbol{t_m}$ the mechanical time constant. The Equation (3.32) can be simplified to a first-order model expressed as follows:

$$\boldsymbol{G_u(s) = \frac{K_T}{r_a B_v + k_e K_T} \frac{1}{s t_m + 1}} \quad (3.34)$$

The corresponding system structure diagram is illustrated in Figure 0.12. Furthermore, the step response of the system described by Equation (3.34) can be expressed as follows:

$$\boldsymbol{\Omega(t) = \frac{K_T U_d}{r_a B_v + k_e K_T} (1 - e^{-t/t_m})} \quad (3.35)$$

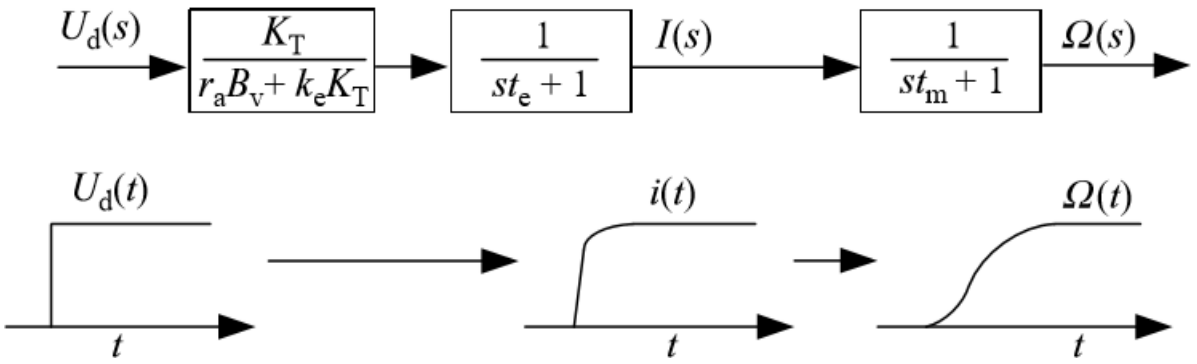


Figure **3.10:** The Speed response of the BLDC motor

As illustrated in Figure 0.11, a smaller mechanical time constant leads to a shorter settling time for the rotor speed Ω(t). In speed control systems, it is desirable for the motor speed to respond quickly with minimal delay. When the mechanical time constant is relatively large, appropriate control strategies must be implemented to improve the system's response speed. For example, in analog control systems, increasing the gain of a voltage or current amplifier can enhance the open-loop gain. Similarly, in digital control systems, increasing the proportional gain of a PI controller can achieve a comparable effect. These approaches help reduce the rise time of the speed response.

In the section, the transfer function and speed step response of brushless dc motor under in the nonzero lto the oad torque will be analyzed. In this case, the load torque is treated as an input disturbance to the system, as illustrated in Figure 0.11.

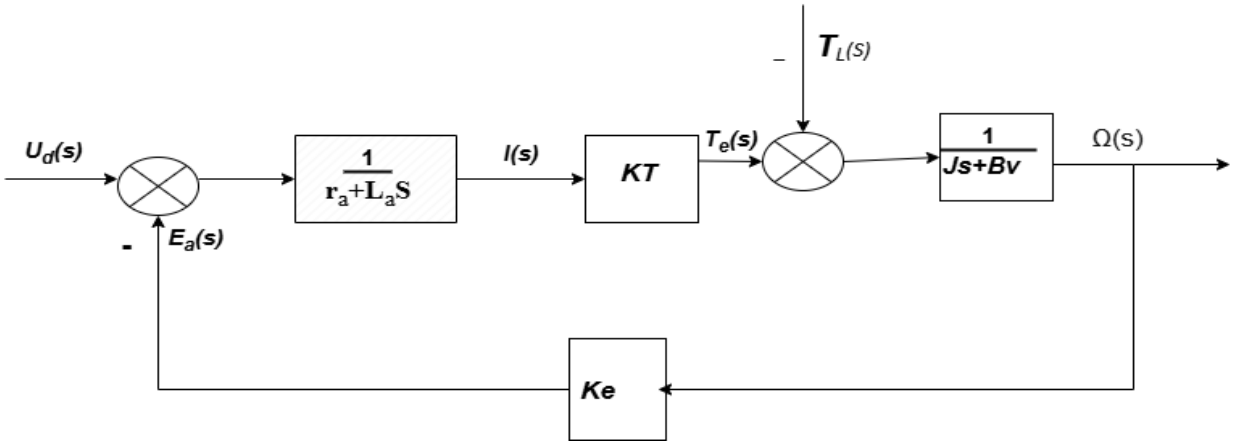


Figure 3.11 The Brshless dc motor with load torque.

For this type of system, the principle of the superposition applies . Therefore, the overall system output is equal to the sum of the individual outputs produced when the Ud(s) and TL(s) are applied separately. As illustrated in Figure 0.12, if Ud(s)=0, then the system response is determined solely by the load torque input, TL(s), and can be expressed as:

$$[-k_e \frac{1}{r_a+L_a s} K_T \Omega(s) - T_L(s)] \frac{1}{Js+B_v} = \Omega(s) \quad (3.36)$$

So

$$\Omega(s)[\frac{(r_a+L_a s)(Js+B_v)+k_e K_T}{(r_a+L_a s)}] = -T_L(s) \quad (3.37)$$

The function of the transfer function to the representing the same character between the load torque and the motor speed can be expressed as follows:

$$G_L(s) = \frac{\Omega(s)}{T_L(s)} = -\frac{r_a+L_a s}{L_a J s^2+(r_a J+L_a B_v)s+(r_a B_v+k_e K_T)} \quad (3.38)$$

Therefore, the speed response of a BLDC motor affected together by voltage and load torque is given by

$$\Omega(s) = G_u(s)U_d(s) + G_L(s)T_L(s)$$

$$= \frac{K_T U_d(s)}{L_a J s^2+(r_a J+L_a B_v)s+(r_a B_v+k_e K_T)} - \frac{(r_a+L_a s)T_L(s)}{L_a J s^2+(r_a J+L_a B_v)s+(r_a B_v+k_e K_T)} \quad (3.39)$$

3.6.2 Stability analysis Permeant magnet brushless DC motor

The PMBLDC motor plant in open-loop (no controller) using the exact second-order transfer function derived from your parameters.

$$G(s) = \frac{Y(s)}{U(s)} = \frac{K_T}{L_a J s^2+(r_a J+L_a B_v)s+(r_a B_v+k_e K_T)}$$

Table 0.2 Parameter of Permanent Magnet Brushless Dc Motor [31]

No.	Description	Symbol	Rating value	Unit

1	Poles of motor	P	4	
2	Resistance per phase	i_a	0.7	Ω
3	Self-inductance per phase	La	0.00521	H
4	Back-EMF coefficient	K_e	0.0143	V/rpm
5	The torque coefficient	K_t	0.1365	v/rad
6	Moment of inertia	J	0.0022	kg/m^2
7	Viscous friction coefficient Be	B_v	0.0002	Nm/rad/sec
8	Rated speed	N	4000	Rpm
9	Rated current	I	8.5	A
10	Maximum permissible torque	Mat	10 2.73	Nm
11	DC link voltage	*V*	380	V

This is the standard second-order transfer function for a PM-BLDC motor (or DC motor equivalent) from armature voltage $u_d(s)$ to angular speed ω(s).

Analyze the model dynamic of a Permanent Magnet BLDC, motor

Let me derive it step by step using the Laplace transform to confirm it matches analysis Electrical and Mechanical characteristic your notation and parameters.

Step 1: Motor Equations

Electrical equation (armature circuit):

$$u_d = r_a i_a(t) + L_a \frac{di_a(t)}{dt} + ke\omega(t)$$

where:

$u_d =$ The dC bus voltage

$r_a =$ The resistance per phase of the winding

L_a= The Self-inductance per phase of the winding

i_a= The armature current

ke= back –EMF constant

Mechanical equation (torque balance):

$$K_T i_a(t) = J\frac{d\omega(t)}{dt} + Bv\omega(t$$

Where

K_T=torque constant

J=moment of inertia

Bv=viscous friction coefficient

Step 2: Apply Laplace Transform (Zero Initial Conditions)

Assume zero initial conditions: $i_a(0) = 0$ ω(0)=0

Electrical equation (s domain) or Laplace domain

$$U_d(s) = raIa(s) + LaSIa(s) + Ke\,\Omega(s)$$

$$U_d(s) = (r_a + LaS)Ia(s) + ke\,\Omega(s$$

$$Ia(s) = \frac{Ud(s) - ke\Omega(s}{ra + Las}$$

Mechanical equation

$$K_T Ia(s) = JS\,\Omega(s) + Bv\,\Omega(s)$$

$$K_T\, Ia(s) = (JS + Bv)\,\Omega(s$$

$$Ia(s) = \frac{(JS+Bv)\Omega(s)}{kT}$$

- KT- is the torque constant,
- Ia - is the armature current in the Laplace domain,
- J= represents the rotor moment of inertia,
- Bv - denotes the viscous friction coefficient, and
- Ω(s) -is the angular speed of the motor.

Step 3 substitute the two question

Substitute the expression for $Ia(s)$ from the mechanical equation into the electrical equation:

$$U_{d(s)} = (r_a + L_a s) \cdot \frac{(JS+Bv)\Omega(s)}{kT} + Ke\,\Omega(s)$$

Multiply through by KT to clear the denominator:

$$K_T U_{d(s)} = (r_a + L_a s)(J s + B_v)\Omega(s) + k_e K_T \Omega(s)$$

Expand the product:

$$(r_a + L_a s)(J s + B_v) = r_a J s + r_a B_v + L_a J s^2 + L_a B_v s$$

$$= L_a J s^2 + (r_a J + L_a B_v)s + r_a Bv$$

So the equation becomes:

$$K_T U_{d(s)} = [L_a J s^2 + (r_a J + L_a B_v)s + r_a B_v + k_e K_T]\,\Omega(s)$$

Step 4: Solve for the Transfer Function

$$\frac{Y(s)}{U(s)} = \frac{K_T}{LaJ s^2 + (r_a J + L_a B_v)s + (r_a B_v + k_e K_T)}$$

his is exactly the form you provided

$$G(s) = \frac{K_T}{LaJ s^2 + (r_a J + L_a B_v)s + (r_a B_v + k_e K_T)}$$

The given BLDC motor parameter find TF above formula

A = $\boldsymbol{LaJ = 0.00521 \times 0.0022 = 1.146 \times 10^{-5}}$

b = $\boldsymbol{raJ + LaBv = (0.7)(0.0022) + (0.00521)(0.0002) = 1.544 \times 10^{-3}}$

C=$\boldsymbol{raBv + keKT = (0.7)(0.0002) + (0.1365)(0.1365) = 1.877 \times 10^{-2}}$

The transfer function in

$$\boldsymbol{TF = \frac{0.1365}{1.14610^{-5}s^2 + 0.001541s + 0.01880}}$$

The characteristic equation is

= $1.146\times10^{-5}s^2+0.001541s+0.01880 =0$

For a $\boldsymbol{s^2 + a1s + a0 = 0}$ stable of the system

For stability:

All elements in the first column must be positive

All coefficients have the same sign (i.e., a1 > 0 and a0 > 0)

So all positive the system is asymptotically stable

1. **Open-Loop Step Response of the PMBLDC motor without controller**

$$\mathbf{G(s) = \frac{K_T}{L_a ras^2+(r_aJ+L_aB_v)s+(r_aB_v+k_eK_T)}}$$

$$\mathbf{TF = \frac{0.1365}{1.14610^{-5}s^2+0.001541s+0.01878}}$$

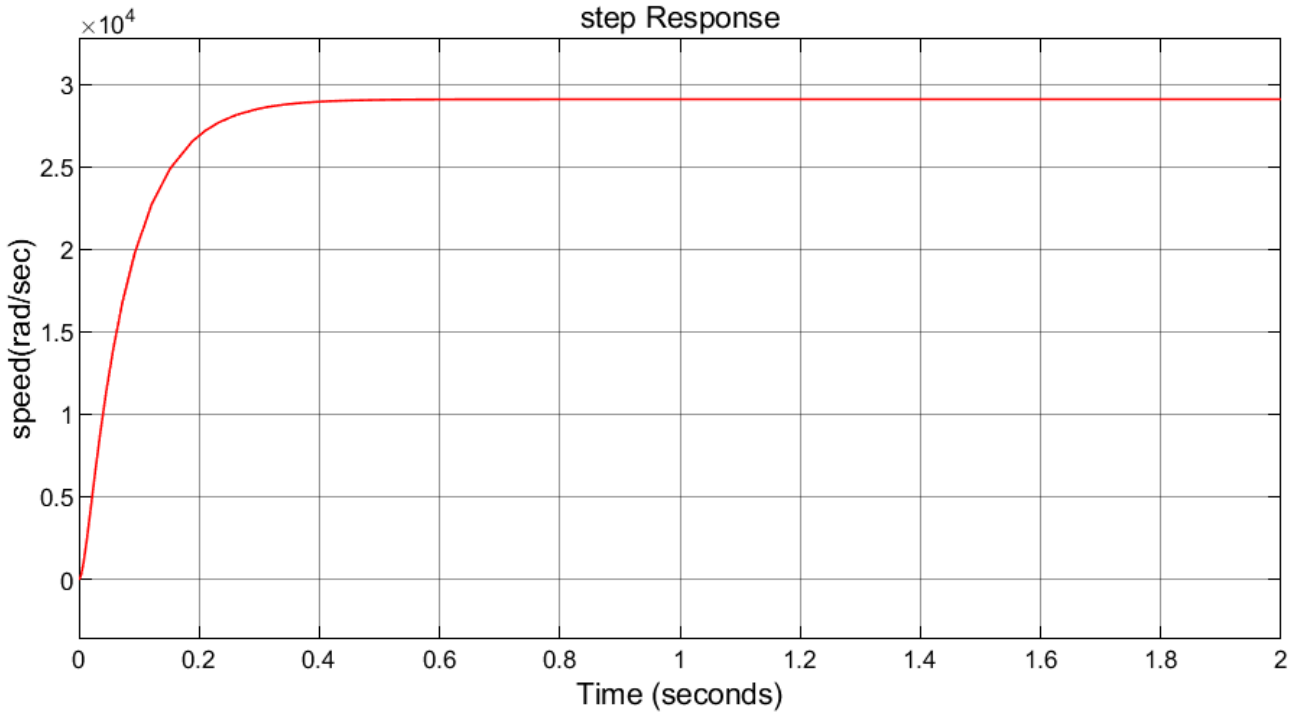


figure 3.12 With out controller permanent Magnet Brushless DC motor response

The step response of the PMBLDC motor without a controller shows a stable and smooth the open-loop behavior. When a step reference input of 4000 rpm is applied, the motor speed rises rapidly and reaches a steady-state value without oscillations or overshoot, indicating inherent stability of the motor dynamics. However, the steady-state speed does not match the reference input, resulting in a large steady-state error. This occurs because, in open-loop operation, the motor speed is determined solely by its electrical and mechanical parameters, particularly back-EMF and losses. Therefore, the PMBLDC motor alone cannot regulate speed accurately, highlighting the necessity of a closed-loop controller.

CHAPTER FOUR

DESIGN OF CONTROLLER

4.1 Chapter Overview

Chapter Four provides an overview of the proposed Model Reference Adaptive Control (MRAC) approach based on Lyapunov stability theory and the MIT rule. This chapter also explains the design procedure of the adaptive controller and its operating principles. In addition, the reference model is developed so that its output can closely follow the output of the plant, which in this case is the Brushless DC (BLDC) motor. The objective is to ensure that the motor output tracks the desired reference model response under different operating conditions.

4.2 Controller Design

4.2.1Adaptive Control Scheme

An adaptive control system is generally defined as a control system capable of modifying configuration of parameter settings, for instance online controls, in response to input. Controllers featuring customizable settings and a mechanism for fine-tuning altering them are also referred to as adaptive controllers. System adaptive control involves two loops: regular feedback with the process and parameter adjustment. Adaptive control methods are extremely beneficial when designing controller with better functionality and performance.[32][33]

4.2.2Model Reference Adaptive Controller

The model reference Adaptive control is a strategy wherein the system's output is derived from a reference model. This approach can be conceptualized as flexible servo system, where the model of the reference delineates. then the reference model expected response to input signal, thereby indicating the intended performance. MRAC controller block diagram is illustrated in Figure 4.1.[34]

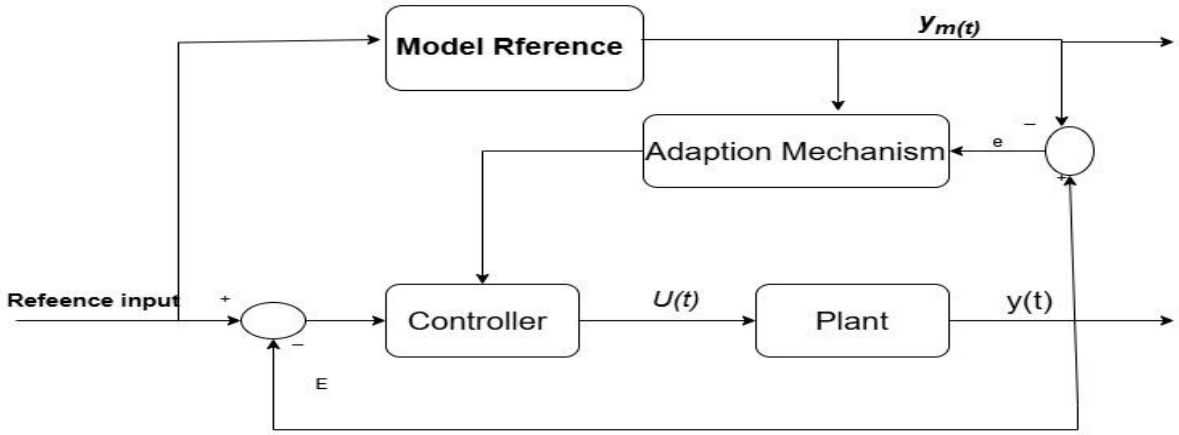


Figure 4.1 Model Reference adaptive control

Two techniques are available for modifying parameters in model reference adaptive control namely, the Gradient approach (MIT rule) and the Lyapunov stability theory.

4.2.3 Design Model Reference Adaptive Control with MIT Rule

The one of the best and most used methods for adjusting parameters in Model Reference Adaptive Control (MRAC) is the gradient approach, also referred to as the MIT Rule. Its foundation is the steepest descent (gradient) approach for minimizing a cost function.

The tracking error is defined as the difference between the actual plant output and the reference model output:

$$\mathbf{e = y - y_m} \qquad \textbf{(}4.1\textbf{)}$$

Equation 4.2 defined the function of cost as

$$\boldsymbol{J(\theta) = \frac{1}{2}e^2(t)} \qquad (4.2)$$

MIT Adaptation Law

To minimize the cost function, the controller parameters are adjusted in the direction opposite to the gradient of the cost function with respect to the parameters. The MIT adaptation law is given by:

If θ represents controller parameter vector, the parameter is adjusted to shift the gradient of the square of error in opposite direction.

$$\theta = \quad = -\boldsymbol{\gamma}\frac{\boldsymbol{\delta J}}{\boldsymbol{\delta\theta}} \;=\; -\boldsymbol{\gamma}\frac{\boldsymbol{\delta}\mathrm{e}}{\boldsymbol{\delta\theta}} \qquad (4.3)$$

Where

J = Cost function or objective function

y = Actual plant output model

$\boldsymbol{y_m}$ = Reference model output

e = the error

$\boldsymbol{\theta}$ = is the adaptive controller parameter vector

γ = Adaptation gain

r(t) = Reference input

Since the reference model output does not depend on the controller parameters, the sensitivity derivative becomes**:**

$$\frac{\boldsymbol{\partial e}}{\boldsymbol{\partial\theta}} = \frac{\boldsymbol{\partial y}}{\boldsymbol{\partial\theta}} \qquad (4.4)$$

The MIT rule is the $\frac{\boldsymbol{d\theta}}{\boldsymbol{dt}} = -\boldsymbol{\gamma}\frac{\boldsymbol{\partial e}}{\boldsymbol{\partial\theta}} = -\boldsymbol{\gamma}\frac{\boldsymbol{\partial y}}{\boldsymbol{\partial\theta}}$ (4.5)

The Brushless Dc motor to considered as the second-order system of the transfer function

Plant and Reference Model

The PMBLDC motor is approximated as a second-order system with the following transfer function:

$$\boldsymbol{G(s)} = \frac{\boldsymbol{y(s)}}{\boldsymbol{u(s)}} = \frac{\boldsymbol{a_0}}{\boldsymbol{s^2+a_1S+a_2}} \qquad (4.6)$$

The reference model is chosen as a stable second-order system to specify the desired closed-loop dynamics:

$$G_{\mathrm{m}}(s) = \frac{y_m(s)}{\mathrm{R(S)}} \frac{\omega_{\mathrm{n}}^2}{(s^2+2\xi\omega_{\mathrm{n}}s+\omega_{\mathrm{n}}^2)} \qquad (4.7)$$

where:

$= \omega_{\mathrm{n}}$ is the natural frequency,

$= \xi$ is the damping ratio.

The control law is chosen as: -

$$\mathbf{U(t) = k_1 r(t) - k_2 y(t) - k_3 y\,(t)} \qquad (4.8)$$

where k1, k2 and k3 are adaptive controller gains.

By substituting Equation (4.12) into Equation (4.13), the MIT rule can be applied. In this context, S represents the differential operator. Therefore, the output y(t) can be expressed as follow: By substituting the control law into the plant model, the closed-loop output in the Laplace domain is obtained as:

$$y(s) = \frac{a_0 k1}{s^2(a1+a0+a2)s+(a2+a0k2)}\,\mathbf{R(s)}$$

$$y(s) = \frac{a0k1R(s)}{s^2+(a1+a0+k3)s+a2+a0k2} \qquad (4.9)$$

As the consequence, the error dynamic is

$$\mathbf{e_1} = y - y_m$$

$$\mathbf{y(s)} = \left(\frac{a_0 k1}{s^2+(a1+a0+k3)s+(a2+a_0k2)}\right)R(s) \qquad (4.10)$$

Sensitivity Derivatives and Approximation

The sensitivity derivatives required by the MIT rule are approximated by replacing the unknown plant dynamics with the reference model dynamics:

$$\frac{1}{s^2+(a_1+a_0k_3)S+(a_2+a_0k_2))} = \frac{1}{s^2+2\xi\omega_n s+\omega^2_n} \quad (4.11)$$

Adaptation Law

Using the MIT rule and the above approximation, the adaptation laws for the controller parameters are obtained as:

$$\dot{k_1} = -\gamma_{e(t)} \left(\frac{1}{s^2+2\xi\omega_n s+\omega_n^2} r(t)\right) e(t) \quad (4.12)$$

$$\dot{k_2} = \gamma_{e(t)} \left(\frac{1}{s^2+2\xi\omega_n m+\omega_n^2} y(t)\right) e(t) \quad (4.13)$$

$$k_3 = \gamma_{e(t)} \left(\frac{1}{s^2+2\xi\omega_n s+\omega_n^2} y(t)\right) e(t) \quad (4.14)$$

Sensitivity derivative containing the plant's parameters is equated. If reference model mimics the real plant closely, adjustments can be made to the model's characteristics to align with that of the plant, resulting in subsequent derivative of sensitivity Model of reference employed is represented by the Equation 4.15 below:

$$G_m(s) = \frac{\omega_n^2}{(s^2+2\xi\omega_n s+\omega_n^2)} \quad (4.15)$$

The parameter $\alpha 1$ is introduced in the adaptation gain γ According to the two percent condition for setting time, reference model design is based on $\zeta = 1$ in order to achieve $\omega_n = 80$ rad/s . Consequently, the transfer function of the reference model can be expressed as follows:

$$\mathbf{TF} = \frac{6400}{s^2+160s+6400}$$

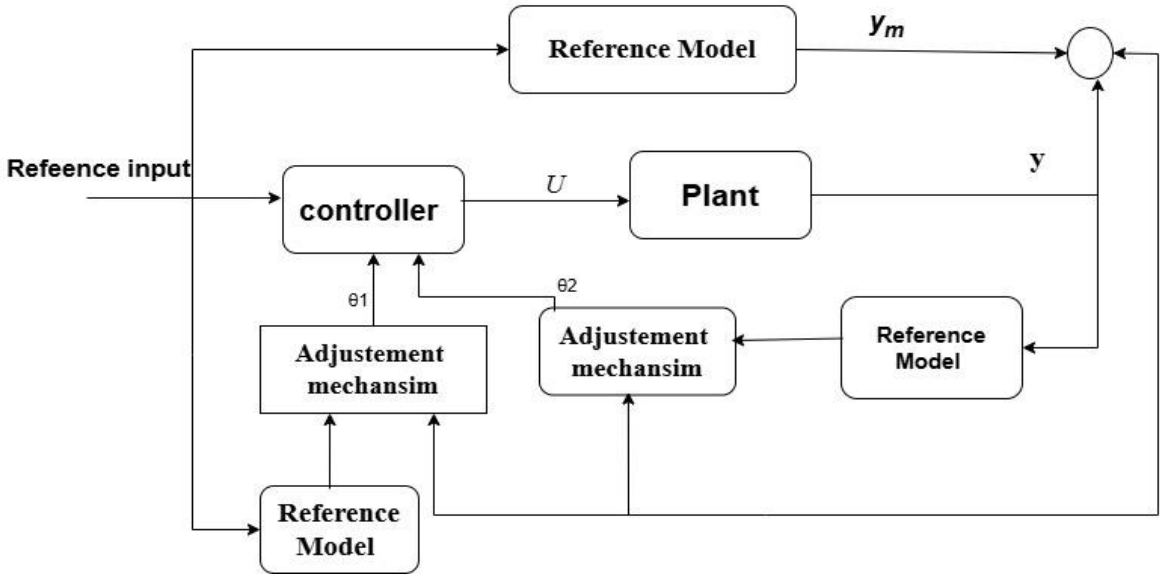


Figure 4.2 The (MRAC) with the MIT rule.

4.2.4 Design of a Model Reference Adaptive Controller Using the Lyapunov Stability Method

The Lyapunov stability theory represents significant technique in adaptive control. Its primary objective is identifying Lyapunov function along with an adaptation method which ensures error between the actual system and the model is minimized to zero.

Considering the PMBLDC motor model of second order.

$$\frac{d^2y}{dt^2} = \text{bu-a}\frac{dy}{dt} \quad (4.25)$$

Furthermore, the Model reference of the second order.

$$\frac{d^2ym}{dt} = b_m r - a_m \frac{dy}{dt} \quad (4.26)$$

Control Law

Consider the input of the controller law as:

$$u(t) = \theta 1 r - \theta 2 y \quad (4.27)$$

Equation 4.28 stated the error as:

$$\text{e} = y - ym \quad (4.28)$$

By inserting Equations 4.25 and 4.26 on Equation 4.28, we obtain

Error dynamics derivation

Taking the second derivative of the error:

$$\ddot{e} = \ddot{y} - \ddot{y}_m$$

$$= -\boldsymbol{a}y - (-\boldsymbol{a}_m y - b_m r) + b_u \quad (4.29)$$

substituting Equation 4.27 on Equation 4.29 results in:

$$\frac{d^2 e}{dt} = a\dot{y} - (-a_m \dot{y} + b_m r) + b(\theta 1 r + \theta \dot{y}) \quad (4.30)$$

The Equation 4.31 is obtained by rearranging the error dynamics between the plant (BLDC motor) and the reference model. It combines terms to express the tracking error ee as:

$$\dot{e} + ame = (am - a_p + bp\theta 1)yp + (bp - bp\theta 2)r. \quad (4.31)$$

This equation presents the second-order error dynamics in a canonical linear form, with two key terms on the right-hand side:

- One term dependent on the plant output y
- One term dependent on the reference input r

Aggregation of analogous terms results:

$$\ddot{e} = -a_m(\dot{y} - \dot{y}_m) + (b\theta 2 + a_m)\dot{y} - b_m * r + b\theta 1 * r \quad (4.32)$$

Equation 4.32 can be rearranged to obtain:

$$\ddot{e} = -a_m \dot{e} - (\dot{a} - \dot{a}_m - b * \theta 2)\dot{y} + (b_m + b\theta 1)r \quad (4.33)$$

Equation 4.33 derived nalyzing the MRAC error dynamics, starting from Equation 4.34

$$\dot{e} = a_m e = b_p(\theta_1 - \theta_1 *)) y_p - b_p(\theta_2 - \theta_2 *))r \quad (4.34)$$

It has been observed from the dynamics of error that the tracking error approach zero under certain conditions. It is possible for the error dynamics to approach zero ($\dot{e} + a_m \dot{e} \rightarrow 0$ e˙+ame→0) without requiring ($\theta_1 - \theta_1 *$)) ($\theta_2 - \theta_2 *$) to be zero.

This happens when the two terms on the RHS cancel each

other out dynamically

Parameter matching conditions

$$\boldsymbol{b\theta_2}* \quad = -a + a_m \tag{4.35}$$

$$b\boldsymbol{\theta_1}* = \boldsymbol{b_m} \tag{4.36}$$

Employ function of Lyapunov to address dynamic error.

It is designed to ensure the structure ensures $V \dot{} \leq 0$, proving stability via Lyapunov theory and parameter convergence.

$$\boldsymbol{V(e,\theta_1,\theta_2)} = \frac{\left(\frac{1}{b\beta}\left(b\theta 1 - bm\right)^2 + e^2 + \frac{1}{b\beta}(b\theta 2 - a_{m+a)^2}\right)\right)}{2} \tag{4.37}$$

We consider $\boldsymbol{V > 0}$

$$\boldsymbol{V(e,\theta_1,\theta_2} = \frac{\left(e^2 + (\frac{-am+a+b\theta 2)^2}{2*b*\beta} + \left(\frac{b\theta 1 - bm^2}{2*b*\beta}\right)\right)}{2} \tag{4.38}$$

Equation 4.38 is a more compact and generalized version of Equation 4.37, useful especially when extending to higher-dimensional parameter vectors. It's a standard step in Lyapunov-based MRAC der Since V is strictly positive for all non-zero values of e, θ~1,θ~2 and zero only at the origin, it is a positive definite function. This property ensures that V is a valid Lyapunov function for proving stability using Lyapunov's direct method.

The expression for differentiation of Lyapunov function provided as:

$$V(e,\theta 1,\theta 2) = \frac{1}{2}e^2 + \frac{1}{2\beta}(-am + b\theta 2 + a)^2 + \frac{1}{2\beta}(-bm + b\theta 1)^2 \tag{4.39}$$

Time Derivative of the Lyapunov function

Differentiate V with respect to time**:**

$$\dot{\boldsymbol{V}} = \boldsymbol{e\dot{e}} + \frac{\boldsymbol{1}}{\boldsymbol{\beta}}(-\boldsymbol{am} + \boldsymbol{b\theta 2} + \boldsymbol{a})\boldsymbol{b\dot{\theta}_2} + \frac{\boldsymbol{1}}{\boldsymbol{\beta}}(-\boldsymbol{bm} + \boldsymbol{b\theta 1})\boldsymbol{b\dot{\theta}_1} \quad (4.40)$$

For stability, V˙ must be negative semi-definite (i.e., V˙≤0V˙≤0).

By inserting value of e into Equation 4.33, we obtain:

For MRAC, the tracking error dynamics are:

$$\boldsymbol{\dot{e}} = -\boldsymbol{ame} + (\boldsymbol{a} - \boldsymbol{am} + \boldsymbol{b\theta 2})\boldsymbol{e} + (\boldsymbol{b\theta 1} - \boldsymbol{bm})\boldsymbol{r}$$

Subsititute in terms of V

$$\dot{V} = -a_m e^2 + e[(a - a_m + b\theta_2)e + (b\theta_1 - b_m)r]$$
$$+ \frac{\boldsymbol{b}}{\boldsymbol{\beta}}(-\boldsymbol{a_m} + \boldsymbol{b\theta_2} + \boldsymbol{a})\boldsymbol{\theta_2} + \frac{\boldsymbol{b}}{\boldsymbol{\beta}}(-\boldsymbol{b_m} + \boldsymbol{b\theta_1})\boldsymbol{\dot{\theta}_1} \quad (4.41)$$

Should these modifications be implemented to the parameter: -

$$\boldsymbol{\dot{\theta}_1} = \ -\boldsymbol{e} * \boldsymbol{\beta} * \boldsymbol{r} \quad (4.42)$$

$$\boldsymbol{\dot{\theta}_2} = \ \ \boldsymbol{e} * \boldsymbol{\beta} * \boldsymbol{\omega} \quad (4.43)$$

The paper successfully demonstrates that Lyapunov-based MRAC ensures stable speed tracking for BLDC motors, outperforming the MIT rule in overshoot and settling time.

The adjustable gain $\boldsymbol{\beta}$ modifies the control parameters, which are θ1 and θ2. The Lyapunov rule block diagram is illustrated in Figure 4.3.

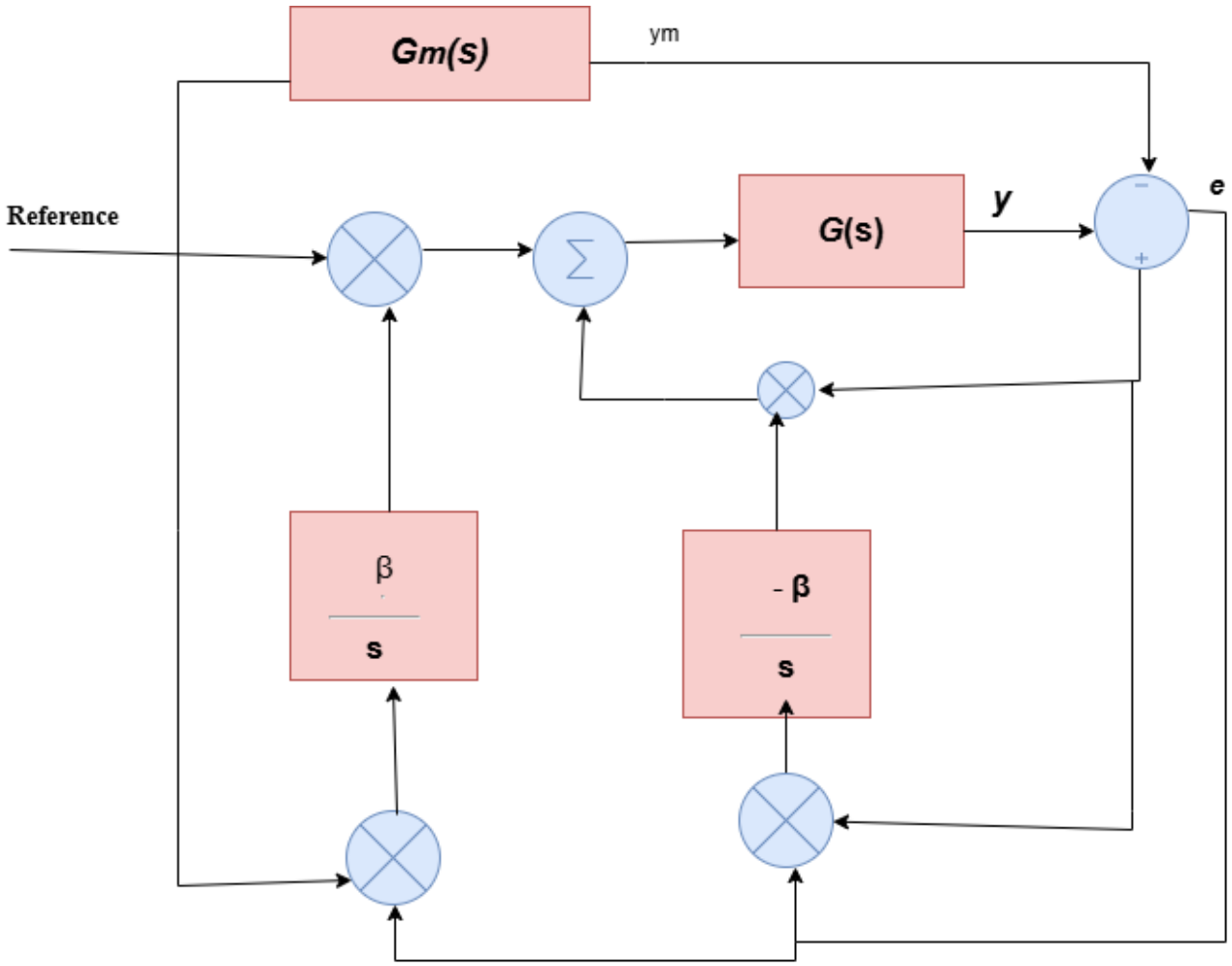


Figure 4.3 MRAC with Lyapunov Stability Method.

4.2.5 Proportional-Integral-Derivative (PID) controller

The Proportional–Integral–Derivative (PID) controller is a widely adopted conventional control strategy in industrial systems. The proportional term responds directly to the current error, delivering immediate corrective action to reduce the deviation from the desired setpoint**.** The integral term responds to the accumulation of past errors, offering a slower response that eliminates steady-state error. The derivative term reacts to the rate of change of the error, helping predict future trends and improving stability. PID controllers can be implemented in both continuous and discrete forms.

In this thesis, the auto-tuning method is preferred because it addresses the limitations of manual PID tuning, which can be time-consuming and prone to error. For speed control of a Permanent Magnet Brushless DC (BLDC) motor, there is no need to manually calculate the controller gains (Kp, Ki, Kd) as required in methods such as Ziegler–Nichols. Instead, the feedback signal can be easily measured and used to automatically adjust the PID parameters. This approach allows the system to achieve a smooth and stable speed response efficiently**.**[35].

. The transfer function of this PID controller is:

$$\boldsymbol{Gc(s) = \ Kp + \frac{Ki}{S} + KdS} \qquad (4.44)$$

$$\boldsymbol{Gc(S) = \frac{Kds^2+KiS+Kp}{S}} \qquad (4.45)$$

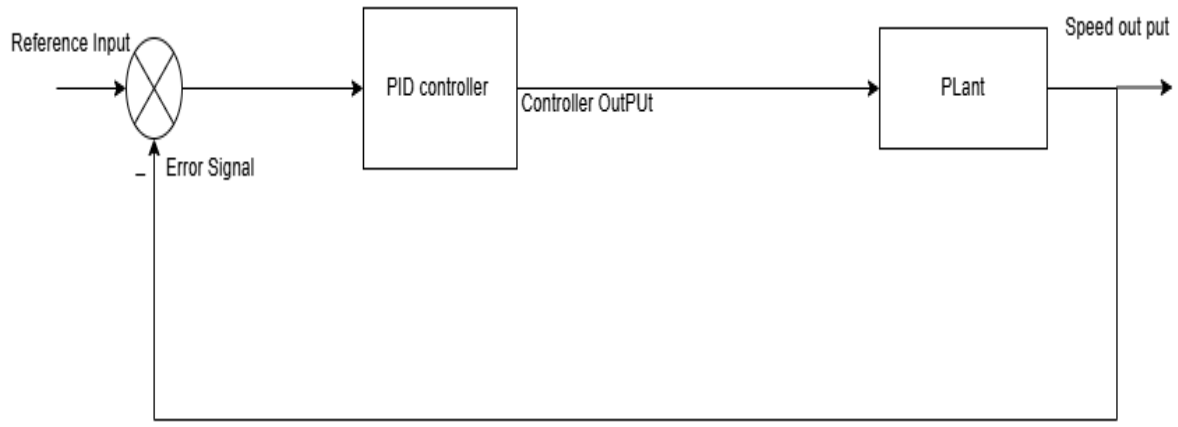


Figure 4.4 : Block diagram of a process control PID controller.

CHAPTER FIVE

RESULT AND DISCUSSION

5.1 Chapter Overview

In this chapter, the numerical parameters used to evaluate the performance of the designed controller are presented, and the simulations were conducted using MATLAB/Simulink R2023b**.** Analysis of simulation findings proposed model reference adaptive controller for speed control of permanent Magnet brushless DC motor . The simulation findings outlined in this section were obtained using the same parameters of the system under investigation.. Also , simulation results of the Permanet Magnate brushless DC motor using control gradient method (MIT rule) , Lyapunov stability method as the MRAC techniques and compare PID controller ,Lyapunov stability are presented. The performance is evaluated based on the transient characteristics of the system, including settling time, overshoot, and rising time. The entire simulation is conducted utilizing MATLAB software.

5.2 Simulation Parameters

During the simulation, the first step is to define the parameters of the Permanent Magnet Brushless DC (BLDC) motor and the load torque. The motor parameters are selected based on values reported in previous studies and journals, ensuring consistency and reliability in the simulation results. The load torque parameters are also specified to represent realistic operating conditions and to evaluate the controller's performance under varying loads**.** [31] as the Table 5.1.

Table 5.1 Simulation parameter of the Permeant magnet brushless Dc motor

No.	Description	Parameter	Rating value	Unit
1	Poles of motor	P	4	
2	Resistance per phase	i_a	0.7	Ω
3	Self-inductance per phase	La	0.00521	H
4	Back-EMF coefficient	K_e	0.0143	V/rpm
5	The torque coefficient	K_t	0.1365	v/rad
6	Moment of inertia	J	0.0022	kg/m^2
7	Viscous friction coefficient Bv	B_v	0.0002	Nm/rad/sec
8	Rated speed	N	4000	Rpm
9	Rated current	I	8.5	A
10	Maximum permissible torque	maxT	10 2.73	Nm
11	DC link voltage	*V*	380	V

As discussed in Chapter Four, based on the chosen reference model criteria, a second-order reference model transfer function was selected. Consequently, the reference model expressed in Equation (4.24) has been adopted for the controller design.

$$TF = \frac{6400}{s^2+160\,s+6400}$$

Dynamics of a closed-loop system were analyzed within the control design portion of this thesis to determine the most suitable reference model. Subsequently, a control law was formulated to achieve the primary control objective of tracking the reference input. It is essential for the reference model to exhibit stability and linearity. Tracking performance result of the reference model is illustrated on Figure 5.1.

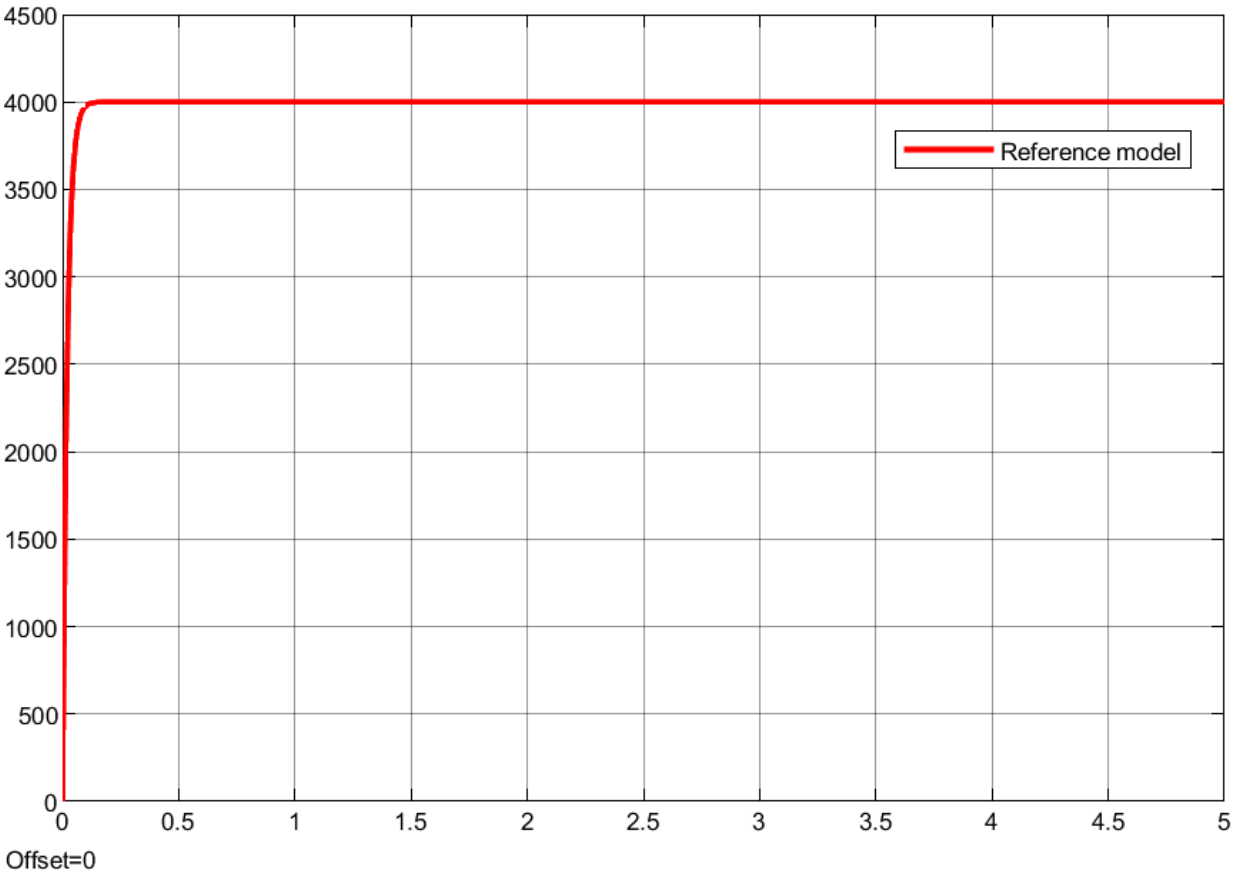


Figure 5. 1 Response model reference for an input reference of 4000rpm

The system exhibits a rise time of 0.04 sec , a settling time of 0.073 sec , a zero overshoot of and zero steady-state error.

5.3 The Performance Analysis

In this chapter, the performance of the Model Reference Adaptive Control (MRAC) scheme using the MIT rule and the MRAC based on the Lyapunov stability approach is evaluated. In addition, a comparative analysis between the conventional PID controller and the Lyapunov-based MRAC is carried out for reference speed tracking at 4000 rpm.

5. 3.1 Proportional- integral -derivative (PID) controller

In this chapter, the parameters of the conventional PID controller are tuned to achieve precise speed tracking and maintain overall system stability in comparison to the open-loop response. The Ziegler–Nichols tuning method is employed to determine the optimal controller gains, effectively addressing issues such as steady-state error, overshoot, and settling time. The resulting PID controller parameters for the speed control system are: Kp=0.21073 , Ki=4.86 and Kd=0.0270 .The step responses of the proposed PID-controlled system are evaluated for a input reference 4000 rpm. In addition, a rated load torque of 0.08 Nm is applied to assess the speed of the controller. The corresponding Simulink model block diagram and simulation results are illustrated in Figure 5.2 and Figure 5.3 respectively.

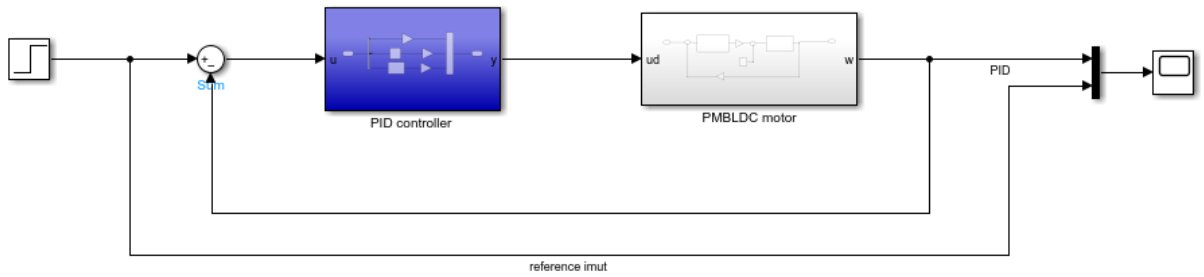


Figure 5.2 Simulink model block PID controller input reference 4000rpm

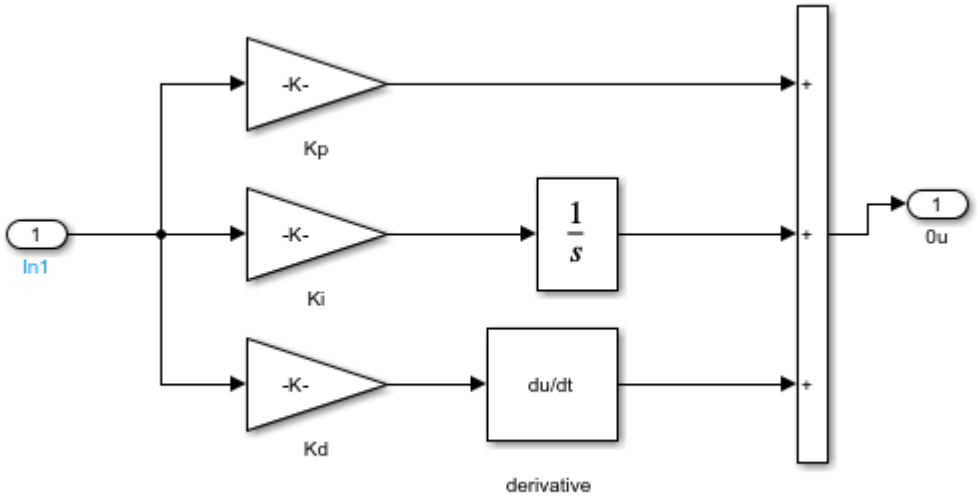


Figure 5.3 Internal PID controller of simulation model

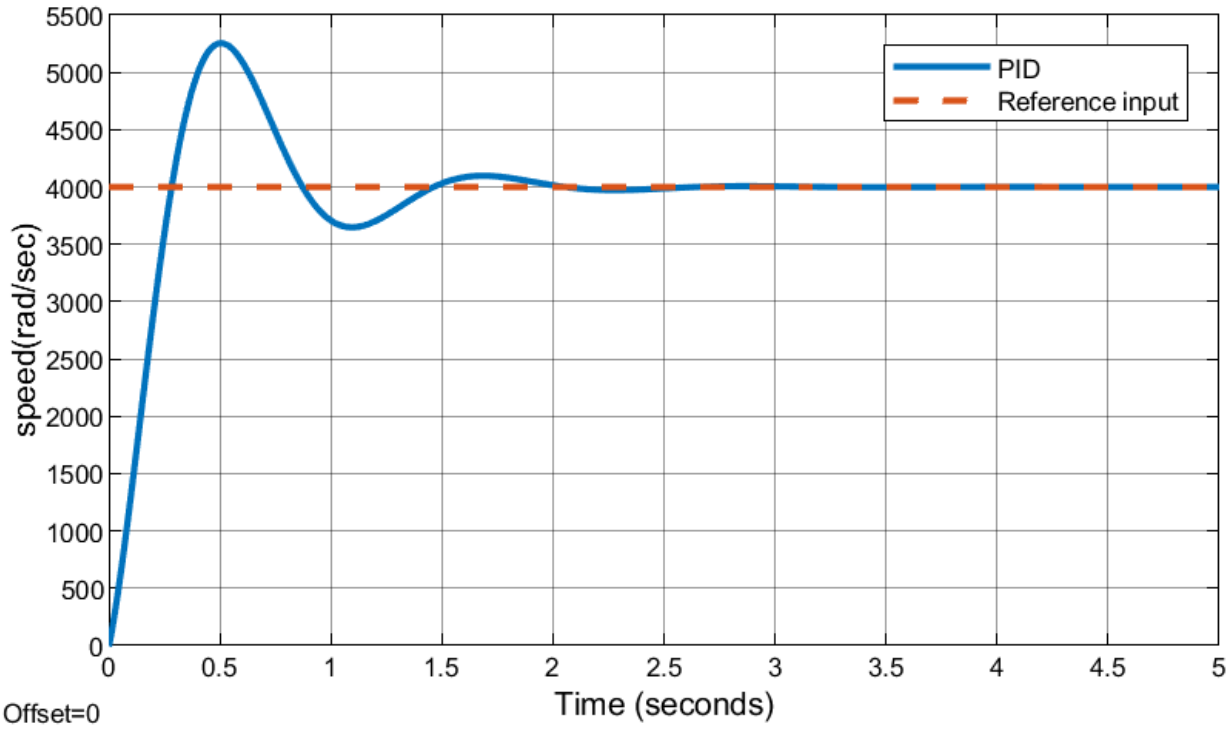


Figure 5.4 Simulink result PID controller Load Torque 0.08 N.m input reference 4000rpm

The figure speed response of the PMBLDC motor using a PID controller was analyzed for a step reference input of 4000 rpm under a load torque disturbance of 0.08 N·m. The simulation shows that the motor accelerates quickly and reaches the desired speed with a very short rise time of 0.2146 sec, and a settling time of 1.8014 secs, demonstrating fast transient characteristics. However, the response exhibits an overshoot of 31.3514%, with a peak speed of approximately 5254 rad/sec before stabilizing at the reference value. This indicates an under-damped behavior caused by aggressive PID gains. Despite the applied load torque, the controller successfully maintains zero steady-state error, showing good disturbance rejection capability. Nevertheless, the large overshoot may cause current surges and mechanical stress, suggesting that further gain tuning is required for smoother and safer operation**.**

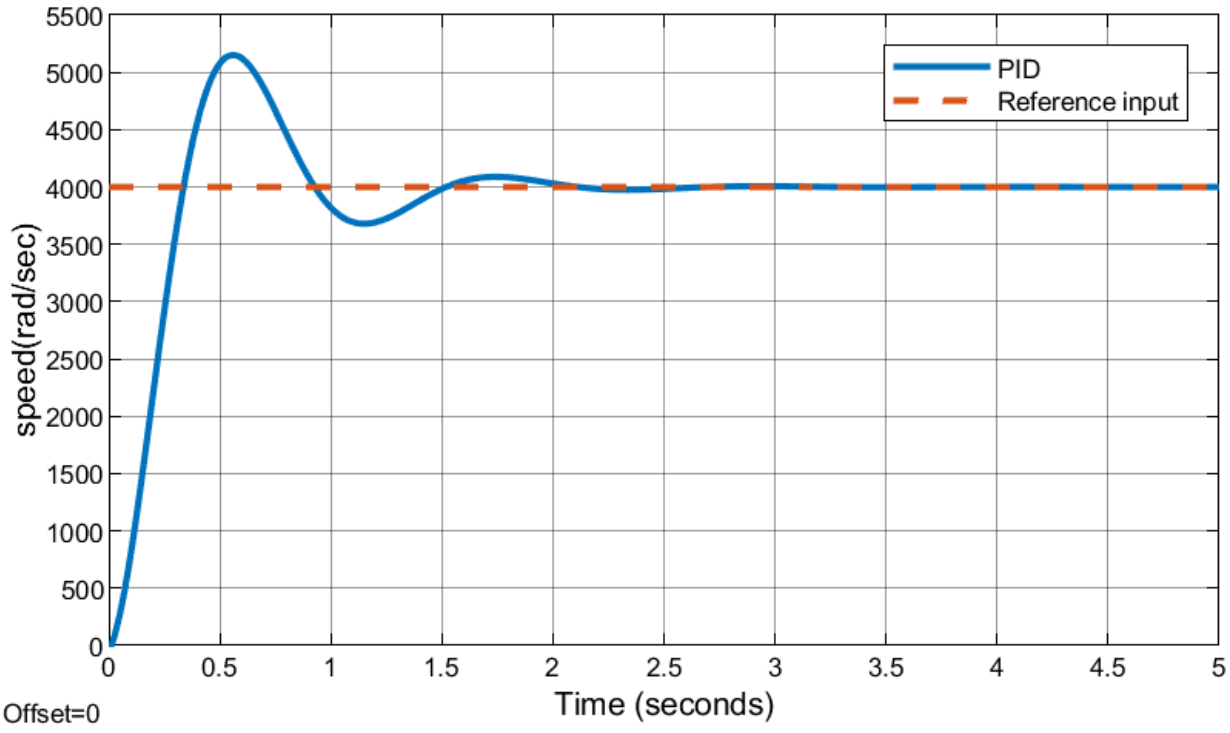


Figure 5.5 Simulink result Load Torque 100N.m input reference 4000rpm

The figure speed response of the PID-controlled PMBLDC motor was evaluated for a reference input of 4000 rpm under a heavy load torque disturbance of 100 N·m. The motor exhibits a fast transient response with a rise time of 0.2389 sec and a settling time of 1.8243 sec, indicating rapid acceleration and stabilization. However, the system shows an overshoot of 28.7676 %, and under overshoot 0.8364, reaching a peak speed of approximately 5151 rad/sec before at the reference value. This behavior reflects an under-damped response due to aggressive PID gains. Despite the large applied load, the controller maintains zero steady-state error, demonstrating good disturbance rejection capability, though further tuning is recommended to reduce overshoot and improve smoothness.

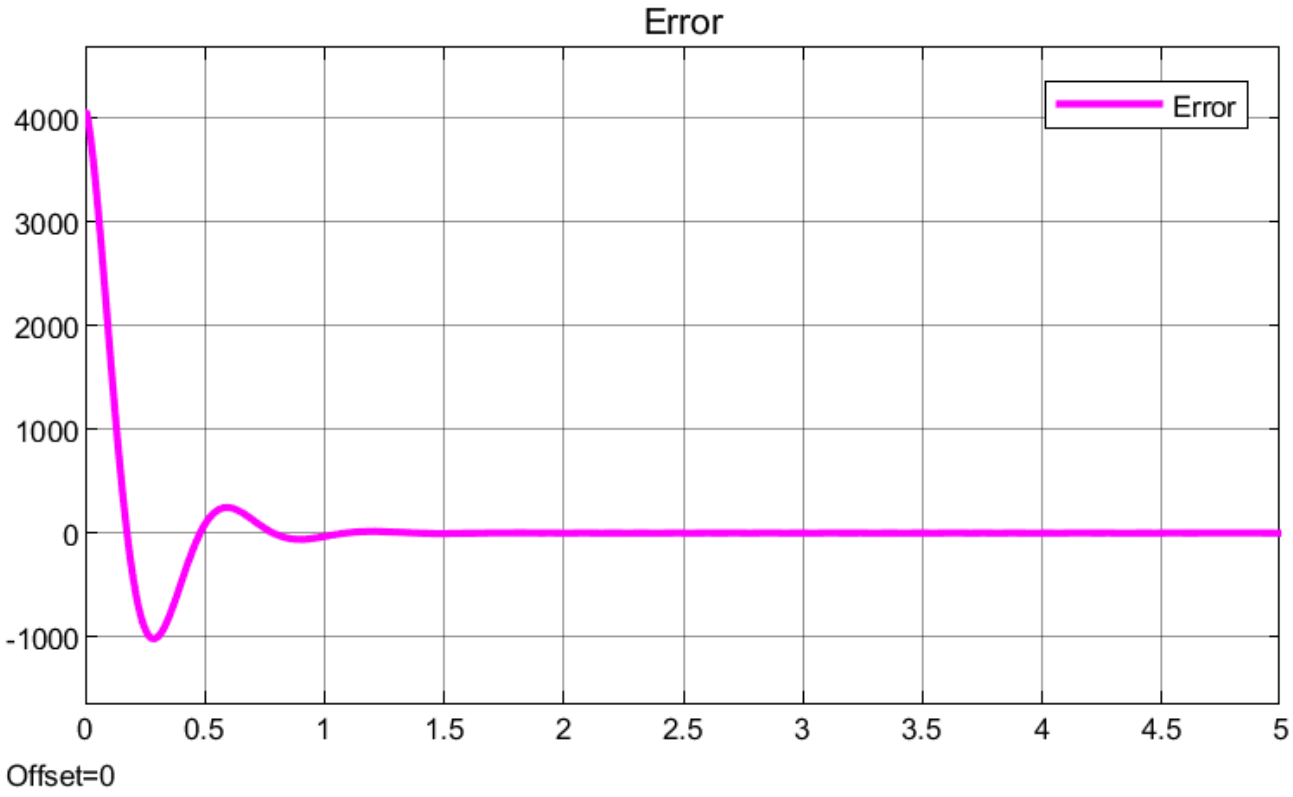


Figure 5.6 Track error signal PID controller

Figure illustrates the tracking error response of the PMBLDC motor speed control system using a conventional PID controller. The initial error is observed due to the difference between the reference speed and the initial motor speed. Once the controller is activated, the error decreases rapidly, indicating an effective proportional and integral control action.

During the transient period, a negative peak followed by a small positive overshoot appears within the first 0.5 s. This behavior reflects the influence of fixed PID gain tuning and the interaction between proportional, integral, and derivative terms. The oscillations are well damped and decay quickly, demonstrating stable closed-loop behavior.

The tracking error converges to zero within approximately 1 s, and no steady-state error is observed for the remainder of the simulation. After the transient period, the error remains essentially zero throughout the remaining simulation time, demonstrating zero steady-state error and stable tracking performance.

This confirms that the PID controller is effective under nominal operating conditions; however, the initial overshoot and oscillatory behavior indicate limited robustness compared to adaptive control strategies when system parameters or load conditions vary.

5.3.2 MRAC with MIT Rule Result

Before the development of alternative adaptive control strategies, the MIT rule was the earliest and most widely implemented technique for adaptive control design. In a Model Reference Adaptive Control (MRAC) scheme based on the MIT rule, the adaptive mechanism continuously adjusts the controller parameters so that the closed-loop system output closely follows the output of a predefined reference model. This is accomplished by formulating a controller with adjustable parameters that are updated to minimize a selected cost function, typically defined in terms of the tracking error. To evaluate the effectiveness of the adaptive gain adjustment, a separate MRAC gradient-based simulation is implemented using Simulink, enabling systematic redesign and performance assessment of the adaptive controller gains.

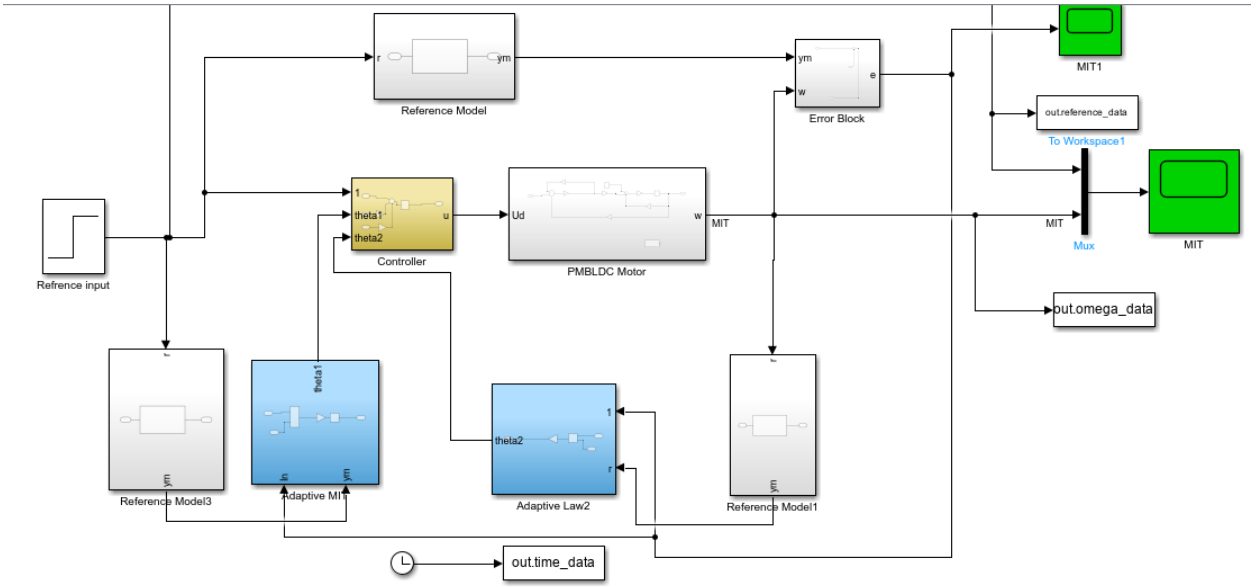


Figure 5.7 The MATLAB/Simulink block diagram of MRAC with MIT rule.

.

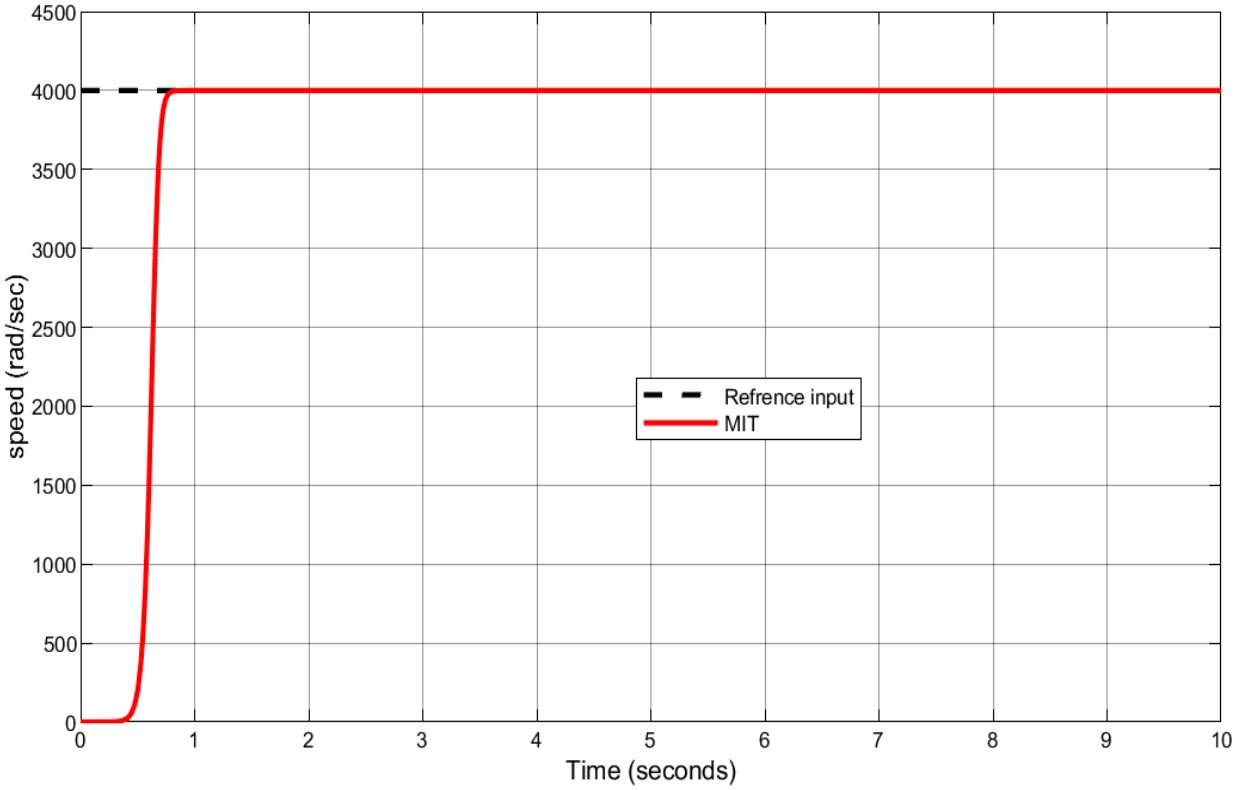


Figure 5.8 Response of PMBLDC Motor Load Torque 0.05 N·m MIT Rule input reference 4000rpm.

This simulation result demonstrates the effectiveness of Model Reference Adaptive Control (MRAC) using the MIT rule for speed control of a PMBLDC motor under a load torque of 0.05 N·m. The motor speed closely follows the reference input of 4000 rad/s with a very fast rise time and smooth transient response. The adaptive controller successfully compensates for the applied load disturbance, achieving zero steady-state error and stable operation without oscillations or overshoot. These results confirm that the MIT-based MRAC scheme provides robust and accurate speed regulation for the PMBLDC motor, making it suitable for high-performance industrial drive applications.

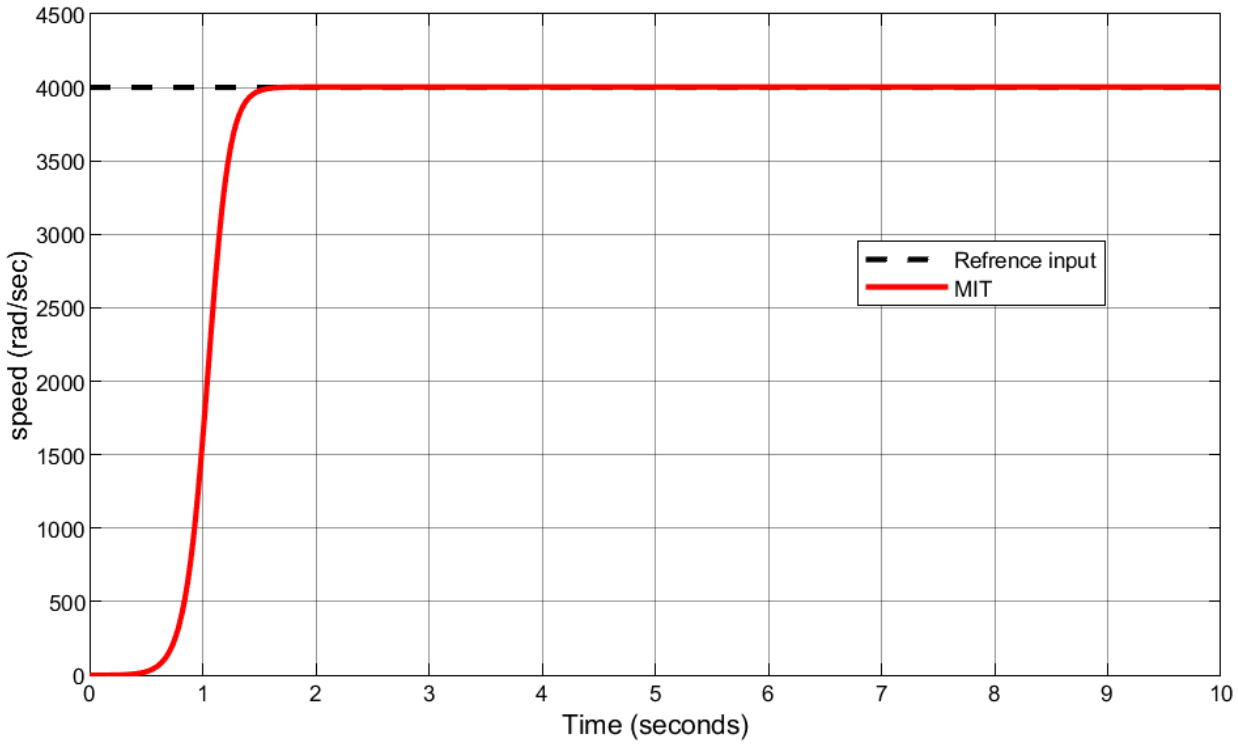


Figure 5.9 Response of the system under Load Torque 0.08 N.m conditions using MIT rule input reference 4000rpm.

The closed-loop speed control simulation results are illustrated in Figure 5.9. The system exhibits a rise time of 0.4392 sec , which is considered satisfactory for the given operating conditions. The settling time and transient time are both 1.3899 s, indicating stable convergence of the speed response. In addition, the system shows a very small overshoot of zero with no undershoot, reflecting excellent damping characteristics. Overall, the controller performance obtained using the MIT rule–based Model Reference Adaptive Control (MRAC) is acceptable, with improved transient behavior and negligible overshoot. These results demonstrate enhanced stability compared to earlier configurations, although further refinement using alternative MRAC methodologies can be considered for performance optimization

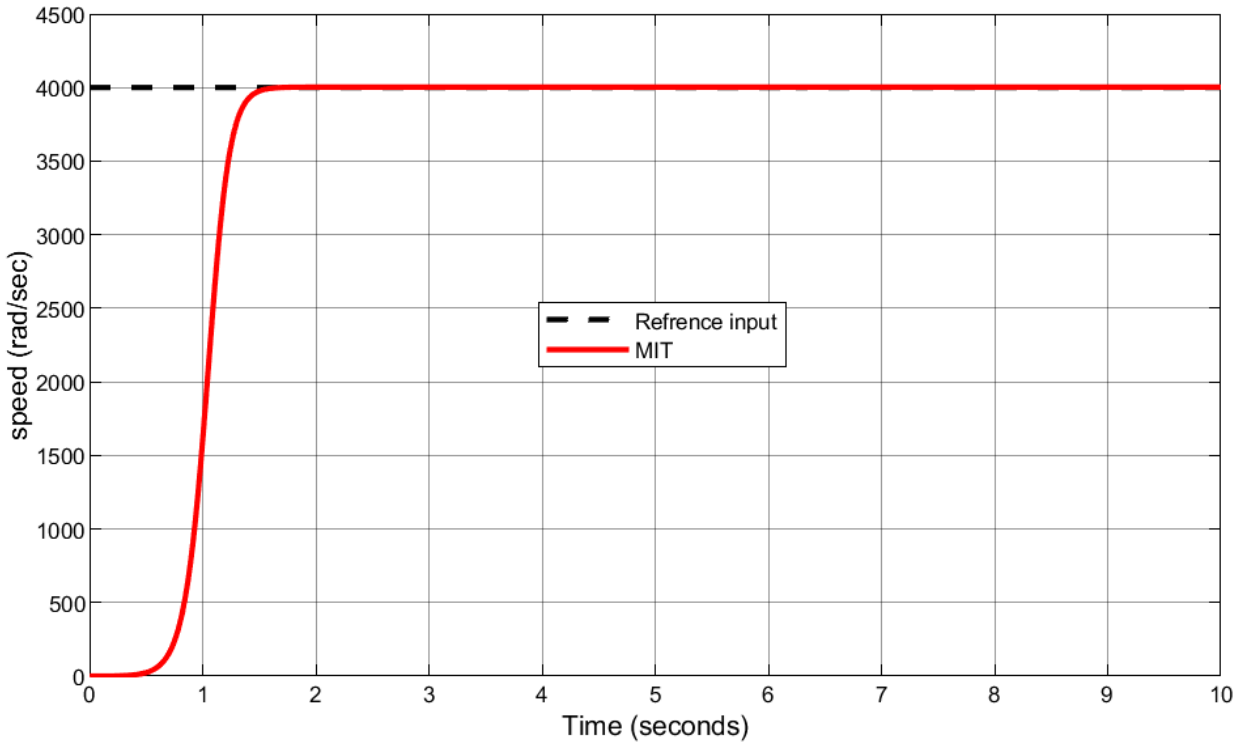


Figure 5.10 Response of Load Torque 100 N.m MRAC with MIT Rule input reference 4000rpm

The simulation results demonstrate that the MRAC with MIT rule provides speed tracking performance for the PMBLDC motor. The motor speed closely follows the reference input of 4000 rpm , as shown by the near-perfect overlap between the reference and actual speed responses.

The system exhibits a rise time of 0.439 **s**ec, indicating a rapid response to the command input. The settling time of 1.4016 sec**,** confirms that the system reaches steady-state quickly, reflecting effective adaptive parameter tuning. The overshoot is zero **,** and no undershoot is observed, highlighting the stability and robustness of the MIT-based adaptive law. Overall, the PMBLDC motor, outperforming conventional fixed-gain controllers in terms of adaptability and steady-state accuracy

5.3.3 Model Reference Adaptive control with Lyapunov stability Result

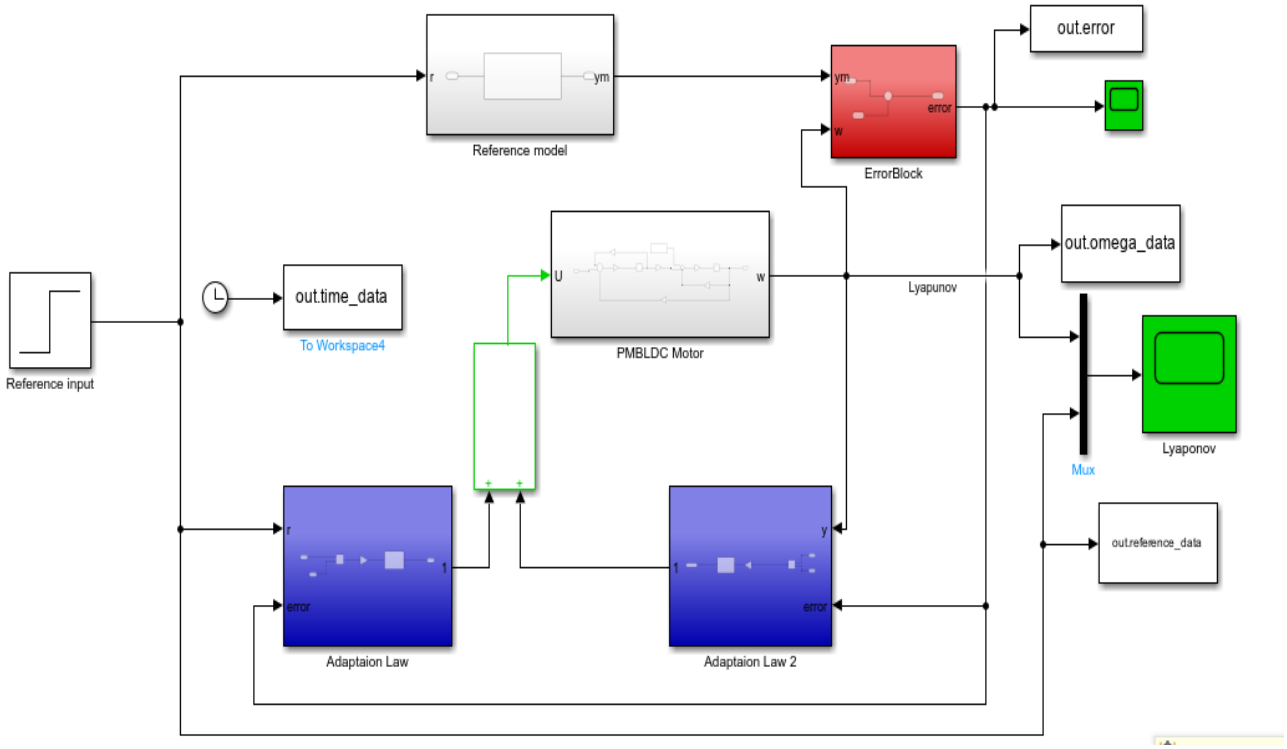


Figure 5.11 MATALB/Simulink model system block MRAC- Lyapunov stability Method

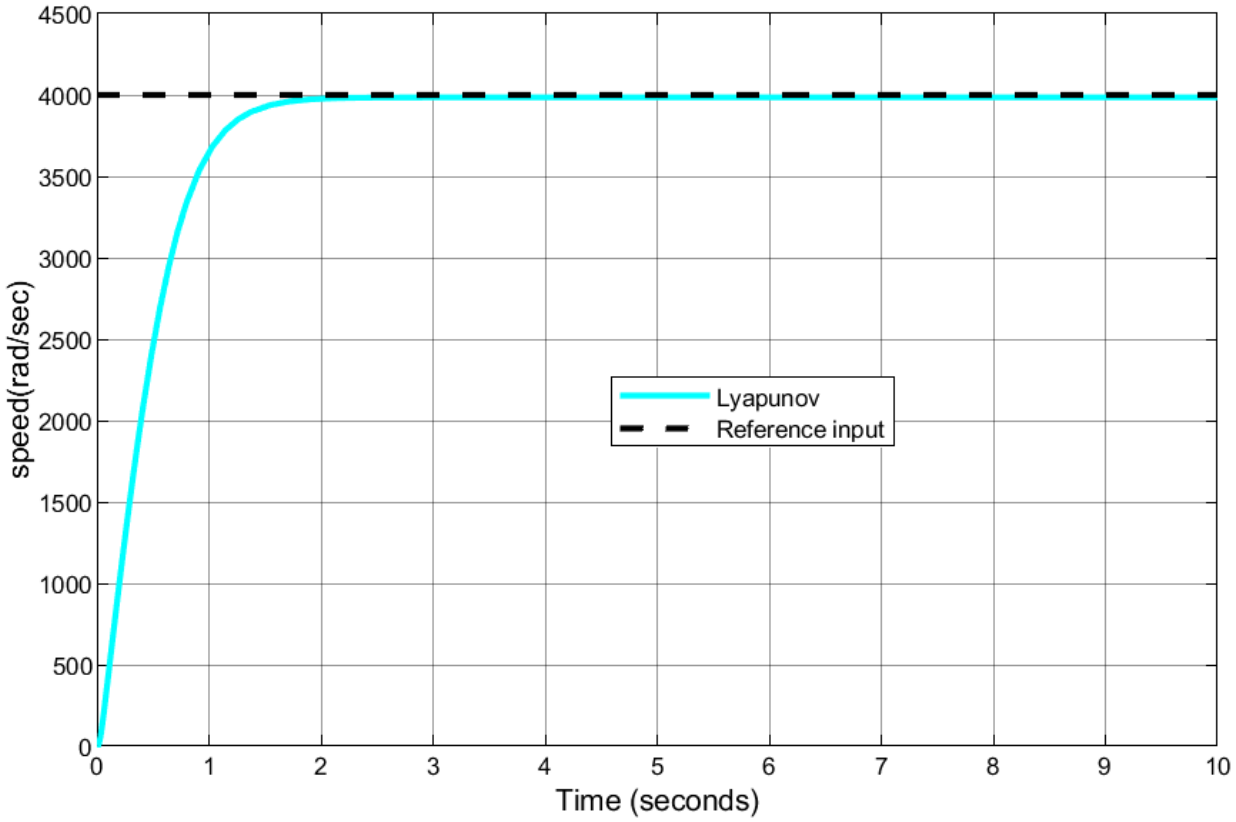


Figure 5.12 Simulink result Lyapunlov no Load torque input reference 4000rpm

This simulation result shows the PMBLDC motor speed response using MRAC with Lyapunov stability for a 4000 rpm reference input under no-load condition.

The motor reaches the desired speed quickly, with a rise time of 0.8972 sec and settles smoothly within 1.49 sec, indicating fast adaptation. The overshoot is zero and no undershoot is observed, confirming excellent damping and closed-loop stability. the Lyapunov-based MRAC provides stable, precise, and reliable PMBLDC motor speed control under no-load operation.

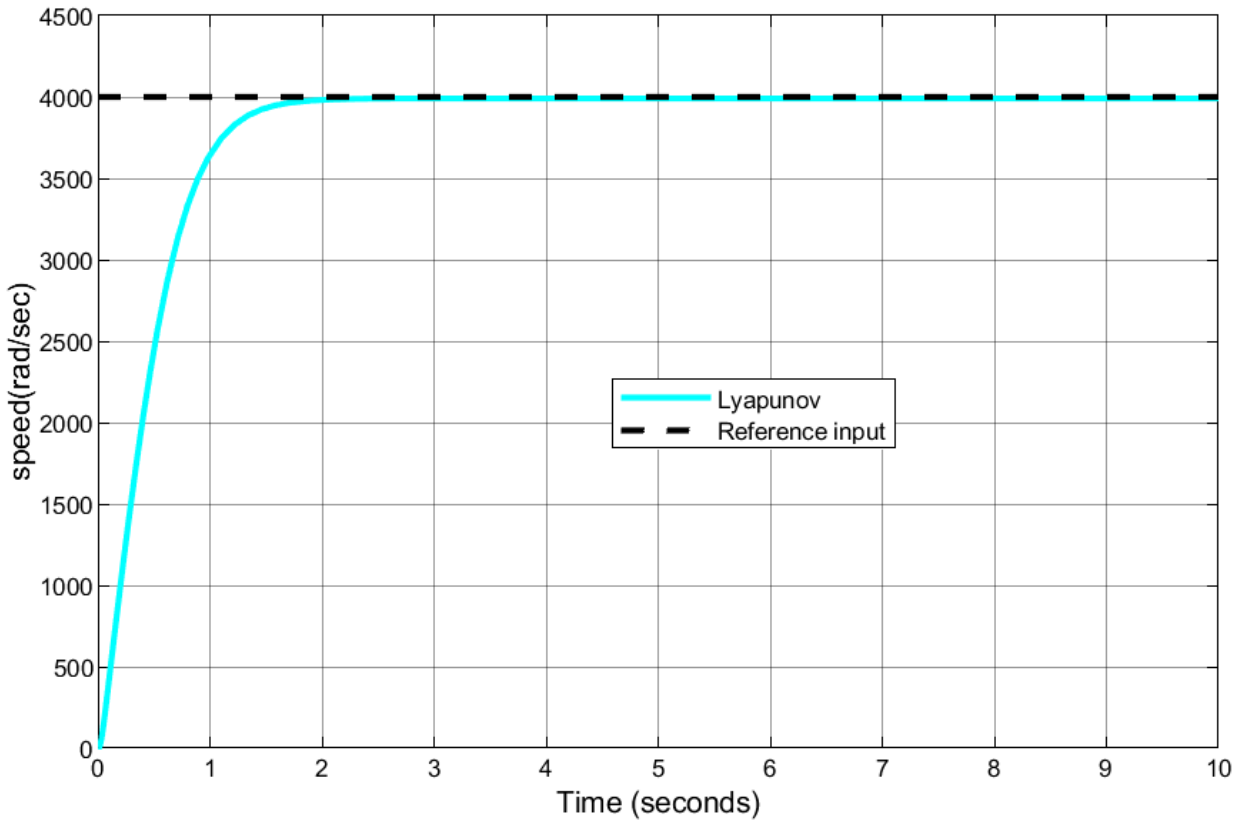


Figure 5.13 Simulink result Lyapunov suitability Load Torque 0.01 input reference 4000rpm

This simulation result confirms the excellent dynamic performance of the PMBLDC motor speed control using MRAC with Lyapunov stability. The motor reaches the reference speed rapidly, with a rise time of 0.8971 **sec,** and settles smoothly within 1.4901 sec, demonstrating fast adaptation. The extremely zero overshoot and negligible undershoot indicate a well-damped response and strong stability margins. The matches the input reference, showing high tracking accuracy. Overall, the Lyapunov-based adaptive controller effectively compensates for system uncertainties and ensures stable, precise, and robust speed control of the PMBLDC motor.

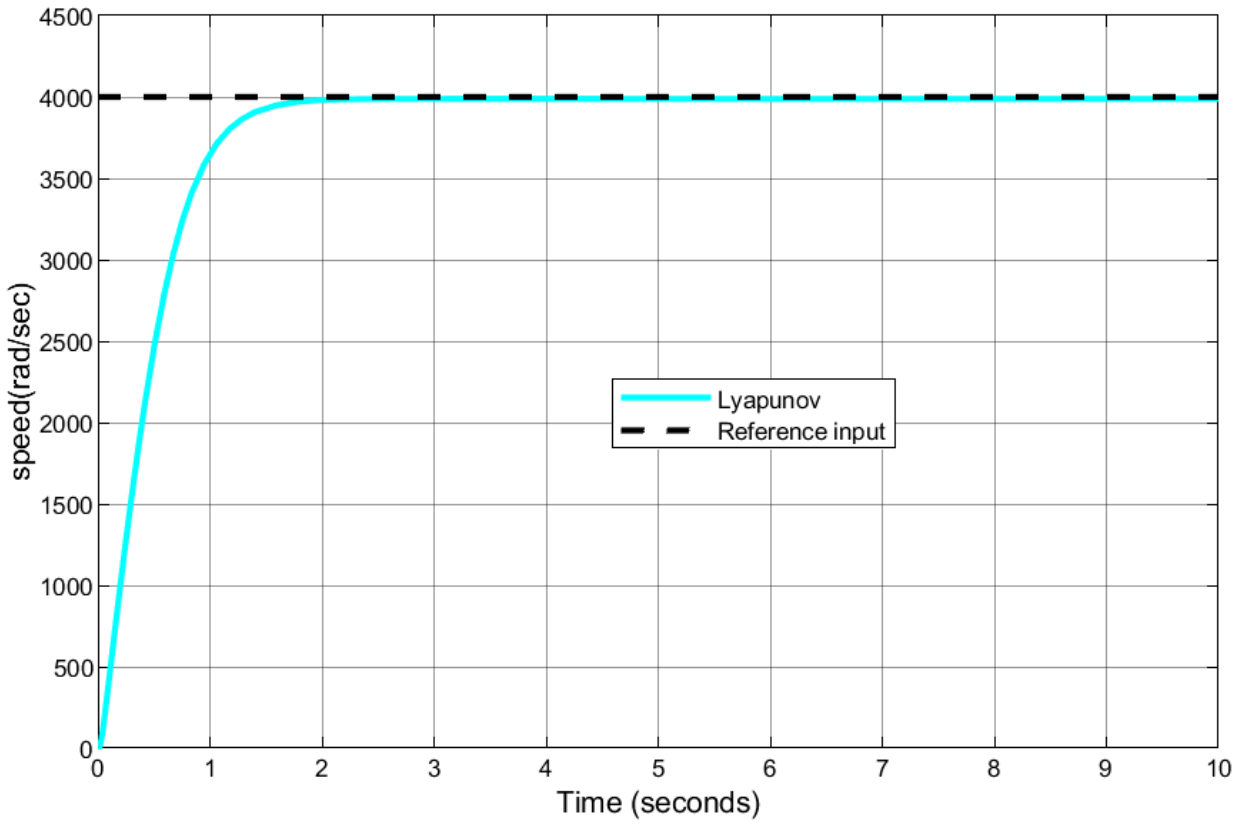


Figure 5.14 Simulink result Lyapunov Load torque 0.08 input reference 4000rpm

These results show very smooth and robust speed control of the PMBLDC motor was MRAC with Lyapunov stability. The motor responds quickly, achieving a rise time of 0.8975 **s** and settling within 1.48 s, which confirms fast adaptive behavior. Overshoot zero **,** and undershoot is practically zero, indicating excellent damping and stable operation. Overall, the Lyapunov-based adaptive controller effectively handles system uncertainties, ensuring precise tracking, minimal oscillation, and reliable dynamic performance suitable for advanced control applications.

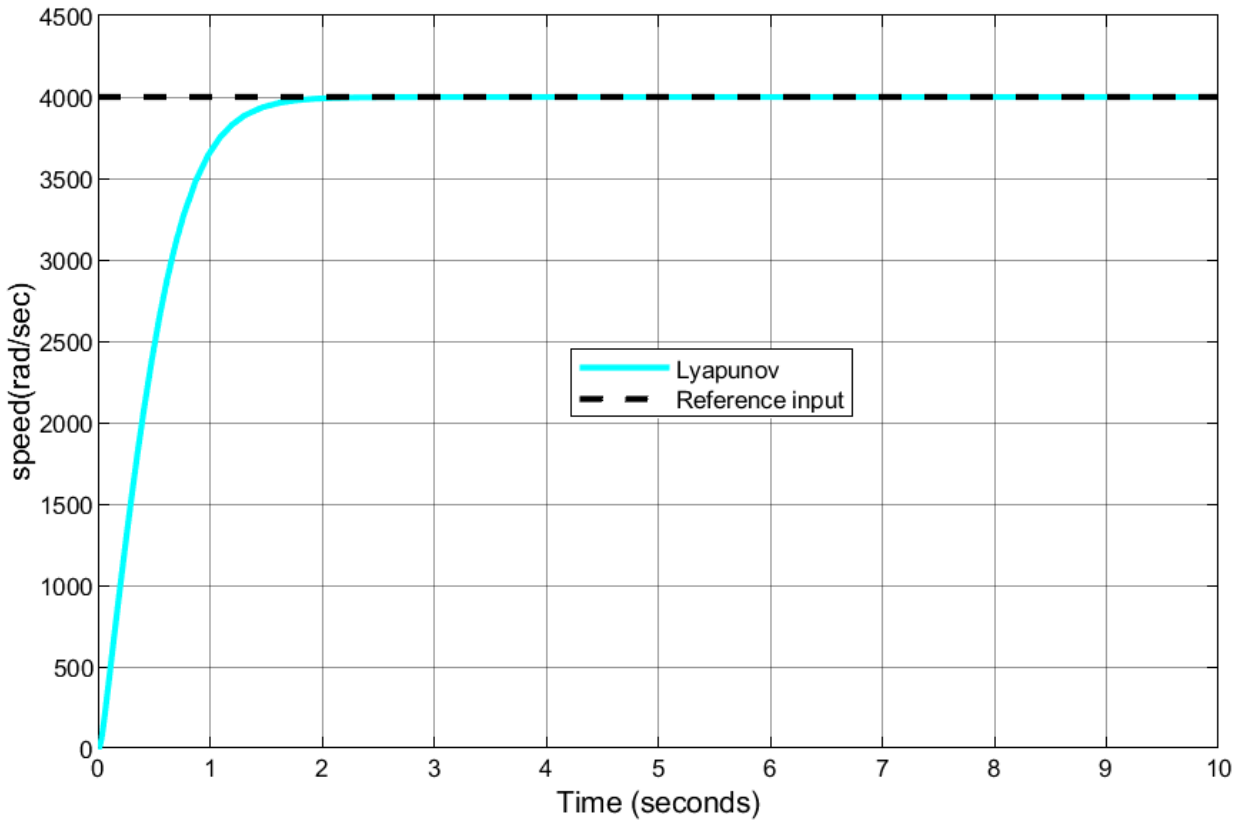


Figure 5.14. Simulink result of Lyapunov stability the Load Torque 100N.m input reference 4000rpm.

The figure illustrates the Simulink simulation result of speed control for a Permanent Magnet Brushless DC (PMBLDC) motor using a Lyapunov stability based adaptive control scheme. The dashed line represents the reference speed input of 4000 rpm, while the solid curve shows the actual motor speed response. From the initial condition, the motor accelerates smoothly and rapidly toward the reference value, indicating effective controller action. The speed response exhibits a fast rise time 0.85sec, settling time 1.41 sec,overshoot zero and steady state zero , demonstrating excellent transient performance. No noticeable oscillations or instability are observed during the transient or steady-state periods. The steady-state speed closely matches the reference input, resulting in negligible steady-state error. The absence of significant overshoot confirms proper damping and well-designed adaptive gain adjustment. According to Lyapunov stability theory, the convergence of the speed error indicates that the closed-loop system is stable and the adaptive parameters are properly regulated. Overall, the simulation results

validate the effectiveness, robustness, and stability of the Lyapunov-based control strategy for PMBLDC motor speed regulation.

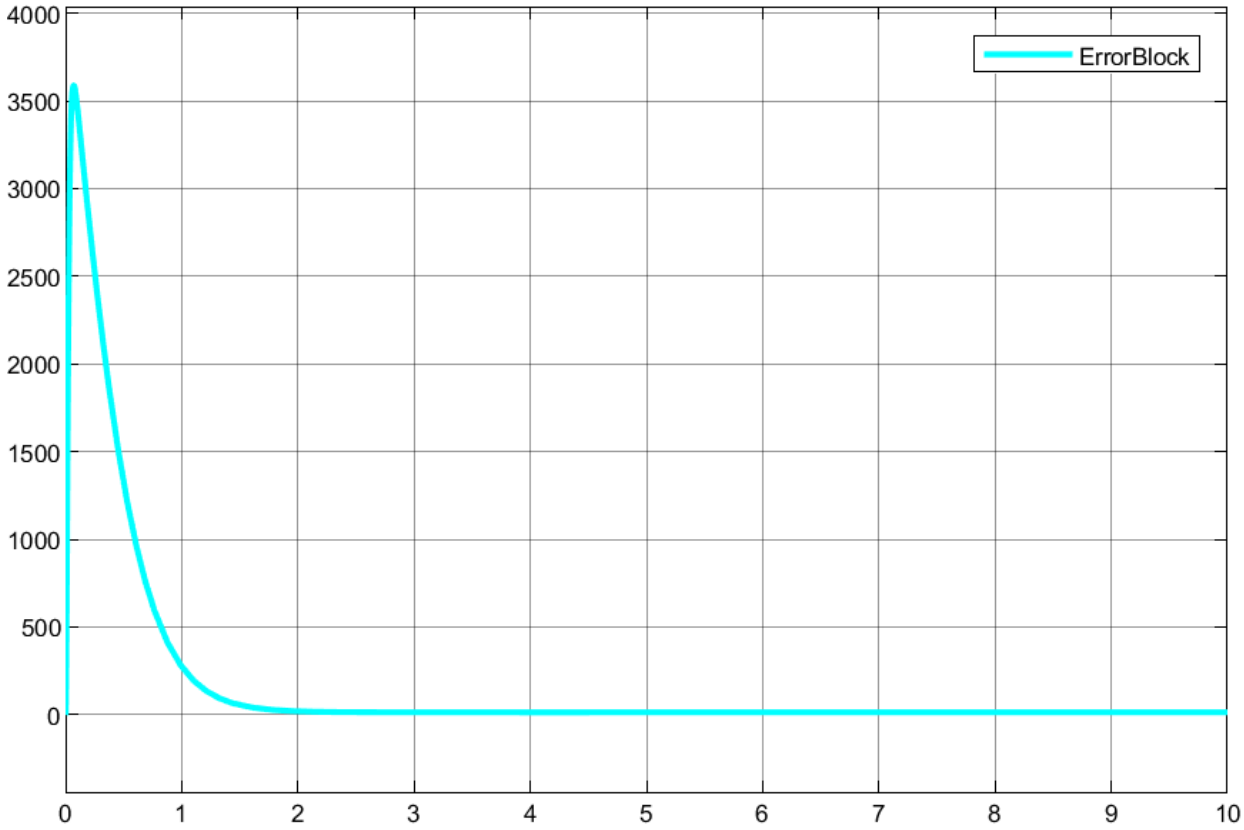


Figure 5.15 Track Error for a Lyapunov-based MRAC speed control of a PMBLDC motor

The figure of the response in the traking error of the PMBLDC motor speed control system employing Model Reference Adaptive Control (MRAC) based on Lyapunov stability theory. The error, defined as the difference between the reference model speed and the actual motor speed, initially exhibits a high magnitude due to the step reference input. However, the error decreases rapidly and converges asymptotically to zero within a short duration. The smooth, non-oscillatory decay of the error confirms that the adaptive law satisfies the Lyapunov stability condition, ensuring a negative semi-definite Lyapunov function derivative. After the transient period, the error remains close to zero, indicating

negligible steady-state error and accurate model tracking. This behavior verifies the closed-loop stability, parameter adaptation, and robustness of the MRAC scheme, demonstrating its effectiveness for high-performance PMBLDC motor speed control under varying operating conditions.

5.3.4 Comparison Between PID Controller and Lyapunov-Based MRAC

A comparison between the conventional PID controller and the Lyapunov-based MRAC scheme highlights their distinct performance characteristics.

The PID controller achieves a riseing time of 0.2146 s and a settling time 1.8014sec. However, it overshoot of 31.3514 % under 0.08 N·m load torque and risng time 0.2389 , settling time 1.8243 and overshoot 28.7676 % Load Torque 100 N·m, indicating under-damped behavior. Although the steady-state error is zero that means effective integral action, the large overshoot may lead to excessive current peaks and mechanical wear, Limited**;** sensitive to parameter changes and load variations

.

In contrast, the Lyapunov-based MRAC exhibits a slower rise time 0.85 -87 s and a settling time of 1.41–1.49 s, but completely eliminates overshoot under all tested load conditions. Even at a heavy load torque of 100 N·m, the controller maintains smooth convergence, negligible steady-state error that means accurate model tracking , and stable operation. The adaptive law derived from Lyapunov stability theory guarantees closed-loop stability and robust performance against parameter uncertainties.

In summary, while the PID controller Limited**;** sensitive to parameter changes and load variations , the Lyapunov-based MRAC provides superior stability, robustness High; adapts to system uncertainties and disturbances , and long-term reliability, making it the preferred control strategy for advanced PMBLDC motor speed control systems.

CHAPTER SIX

CONCLUSIONS AND RECOMMENDATIONS

6.1 Conclusions

This thesis basically investigated the speed control performance of a Permanent Magnet Brushless DC (PMBLDC) motor using, Model Reference Adaptive Control (MRAC) with Lyapunov stability method and the MIT rule, compare a conventional Proportional–Integral–Derivative (PID) controller. All control schemes were designed and evaluated using MATLAB/Simulink under identical operating conditions, with a reference speed of 4000 rpm and load torque disturbances ranging from 0.01 N·m to 100 N·m.

Simulation results show that the PID controller provides the response , with a rise time of 0.2146 sec, and a settling time of 1.8014 sec under a 0.08 N·m load torque. However, the response exhibits a large overshoot of %, reaching a peak speed of approximately 5254 rad/sec . Under a heavy load torque of 100 N·m, the PID controller still maintains zero steady-state error, resing time 0.2389 sec, settling time 1.8243 sec but the overshoot remains high at 28.7676 %, indicating an under-damped response that may cause mechanical stress and increased current demand.

The MRAC scheme based on the MIT rule demonstrates improved robustness and stability. Under a 0.08 N·m load torque, the system achieves a rise time of 0.4392 s and a settling time of 1.3899 s, with zero overshoot and no undershoot. Even under a heavy load torque of 100 N·m, the MRAC with MIT rule maintains accurate speed tracking with a settling time of 1.4016 s and negligible steady-state error. These results confirm that the MIT rule-based MRAC enhances stability and eliminates overshoot; however, its transient response is zero compared to the PID controller.

The MRAC based on Lyapunov stability theory provides the best overall performance. Under no-load conditions, the motor reaches the reference speed with a rise time of 0.8572 s and a settling time of 1.49 s, with zero overshoot. When subjected to load torques of 0.01 N·m, 0.08 N·m, and 100 N·m, the system maintains rise times between 0.85 s and 0.890 s and settling times between 1.41 s and 1.49 s, while

preserving zero overshoot and steady-state error. The tracking error converges asymptotically to zero, confirming closed-loop stability as guaranteed by Lyapunov theory.

Generally the Lyapunov-based MRAC scheme out performs both the PID controller and the MIT rule-based MRAC in terms of stability, robustness, and smooth dynamic response under large load disturbances.

6.2 Recommendations

The recommendations for future work are as follows**:**

- The Lyapunov-based MRAC strategy is highly recommended for PMBLDC motor applications requiring robust operation under large load disturbances with zero overshoot and guaranteed stability.
- Future work should include setting up an experimental testbed and conducting laboratory experiments to validate the simulation results .

Reference

[1] J. F. Gieras, “Design of Permanent Magnet Brushless Motors for High Speed Applications,” 2014.

[2] S. Mallick and U. Mondal, “Comparative performance study of lyapunov based MRAC technique and MRAC augmented with PID controller for speed control of a DC motor,” *2019 2nd Int. Conf. Adv. Comput. Commun. Paradig. ICACCP 2019*, no. 4, pp. 1–5, 2019, doi: 10.1109/ICACCP.2019.8882982.

[3] G. E. Uhlenbeck, “A Modified Lyapunov Method,” 1960.

[4] E. H. Putra, Z. Has, and M. Effendy, “Robust adaptive sliding mode control design with genetic algorithm for Brushless DC motor,” *Int. Conf. Electr. Eng. Comput. Sci. Informatics*, vol. 2018-Octob, pp. 330–335, 2018, doi: 10.1109/EECSI.2018.8752768.

[5] P. A. K. REDDY and R. SRAVANTHI, “Brushless DC motor speed regulation with a fuzzy PID controller,” vol. 13, no. 2, 2023.

[6] S. D. Sahputro, F. Fadilah, N. A. Wicaksono, and F. Yusivar, “Design and implementation of adaptive PID controller for speed control of DC motor,” *QiR 2017 - 2017 15th Int. Conf. Qual. Res. Int. Symp. Electr. Comput. Eng.*, vol. 2017-Decem, no. 1, pp. 179–183, 2017, doi: 10.1109/QIR.2017.8168478.

[7] M. A. Ibrahim, A. K. Mahmood, and N. S. Sultan, “Optimal PID controller of a brushless DC motor using genetic algorithm,” *Int. J. Power Electron. Drive Syst.*, vol. 10, no. 2, pp. 822–830, 2019, doi: 10.11591/ijpeds.v10.i2.pp822-830.

[8] H. Q. Yin, W. J. Yi, C. C. Li, K. J. Wang, and J. T. Wu, “The fuzzy adaptive PID control of brushless DC motor,” *J. Phys. Conf. Ser.*, vol. 1507, no. 5, 2020, doi: 10.1088/1742-6596/1507/5/052005.

[9] M. A. Ramya, S. P. Jadhav, and S. N. Pawar, “Design and Implementation of Particle Swarm Optimization (PSO) Tuned PID Controller for Speed Control of Permanent Magnet Brush Less DC (PMBLDC) Motor,” *2020 Int. Conf. Emerg. Technol. INCET 2020*, pp. 1–6, 2020, doi: 10.1109/INCET49848.2020.9154039.

[10] T. N. Trong, “The control structure for dc motor based on the flatness control,” *Int. J. Power Electron. Drive Syst.*, vol. 8, no. 4, pp. 1814–1821, 2017, doi: 10.11591/ijpeds.v8i4.pp1814-1821.

[11] M. C. Bosco, J. J. Guedes, M. F. Castoldi, A. Goedtel, E. R. Pires Da Silva, and L. F. S. Buzachero, “Estimation of parameters and tuning of a speed PI of permanent magnet DC motor using differential evolution,” *2017 IEEE Int. Electr. Mach. Drives Conf. IEMDC 2017*, 2017, doi: 10.1109/IEMDC.2017.8002318.

[12] H. Suryoatmojo *et al.*, “Robust speed control of brushless dc motor based on adaptive neuro

fuzzy inference system for electric motorcycle application," *Int. J. Innov. Comput. Inf. Control*, vol. 16, no. 2, pp. 415–428, 2020, doi: 10.24507/ijicic.16.02.415.

[13] K. H. Reddy, S. Ramasamy, and P. Ramanathan, "Hybrid adaptive neuro fuzzy based speed controller for brushless DC motor," *Gazi Univ. J. Sci.*, vol. 30, no. 1, pp. 93–110, 2017.

[14] P. K. Khanke and S. D. Jain, "Comparative analysis of speed control of BLDC motor using PI, simple FLC and Fuzzy-PI controller," *Int. Conf. Energy Syst. Appl. ICESA 2015*, no. Icesa, pp. 296–301, 2016, doi: 10.1109/ICESA.2015.7503359.

[15] R. S. Lodhi, P. Salawria, R. Singh Lodhi, and P. Nema, "Implementation of PSO-Based Optimum Controller for Speed Control of BLDC Motor," *Comput. Eng.*, vol. 6, no. 1, pp. 104–109, 2017, [Online]. Available: https://www.researchgate.net/publication/334883660

[16] N. A. Rao and C. R. Kumar, "Speed Control of Brushless Dc Motor by Using PID and Fuzzy Logic Controller," vol. 6, no. 4, pp. 72–77, 2019.

[17] F. Auliansyah, Sutedjo, O. Asrarul Qudsi, and I. Ferdiansyah, "Controlling speed of brushless dc motor by using fuzzy logic controller," *Proc. - 2020 Int. Semin. Appl. Technol. Inf. Commun. IT Challenges Sustain. Scalability, Secur. Age Digit. Disruption, iSemantic 2020*, no. 1, pp. 298–304, 2020, doi: 10.1109/iSemantic50169.2020.9234290.

[18] M. L. Mekha, G. Manju, and P. G. Student, "Speed Control of BLDC Motors Using MRAC," pp. 4–9, 2016.

[19] S. M. A. Motakabber, A. H. M. Z. Alam, A. N. Nordin, and A. K. M. A. Habib, "Modeling and Performance Analysis of an Adaptive PID Speed Controller for the BLDC Motor," vol. 11, no. 7, pp. 272–276, 2020.

[20] A. P. R. Eeb and B. V. Rao, "SPEED CONTROL OF BLDC MOTOR USING ADAPTIVE FUZZY PID CONTROLLER," no. May 2022.

[21] P. S. Vikhe, B. S. Shukla, C. B. Kadu, and V. V Mandhare, "Speed Control of BLDC Motor using Open Loop , PID Controller and Neural Network," no. February, 2020, doi: 10.35940/ijeat.A9710.109119.

[22] R. A. Ardiansyah and E. Yazid, "Rotational Speed Control of Brushless DC Motor Using Genetic Algorithm Optimized PD Controller," vol. 18, no. 2, pp. 75–80, 2018, doi: 10.14203/jet.v18.75-80.

[23] J. Control, F. Adıgüzel, and T. Türker, "A periodic adaptive controller for the torque loop of variable speed brushless DC motor drives with," 2022, doi: 10.1080/00051144.2022.2065802.

[24] H. Abdelfattah, M. I. Mosaad, and N. F. Ibrahim, "Adaptive Neuro-Fuzzy Technique for Speed Control of Six-Step Brushless DC Motor," vol. 9, no. 2, pp. 302–312, 2021, doi: 10.52549/ijeei.v9i2.2614.

[25] J. Control, H. Jigang, F. Hui, and W. Jie, “A PI controller optimized with modified differential evolution algorithm for speed control of BLDC motor speed control of BLDC motor,” vol. 1144, 2019, doi: 10.1080/00051144.2019.1596014.

[26] M. Nguyen, D. Vuong, and T. Nguyen, “The MRAC based - adaptive control system for controlling the speed of direct current motor,” vol. 19, no. 2, pp. 723–728, 2020, doi: 10.11591/ijeecs.v19.i2.pp723-728.

[27] *Permanent magnet brushless dc motor drives and controls*.

[28] I. Introduction, “Modeling, Simulation, and Analysis,” vol. 25, no. 2, 1989.

[29] “PERMANENT-MAGNET BR USHLESS DC KHALID SALIH MOHAMMAD AL-HADITHI for the award of the degree of Doctor ofPhilosophy Of Loughborough University of Technology Al-Hadithi”.

[30] M. A. Kovalenko *et al.*, “MATHEMATICAL SIMULATION OF BRUSHLESS HIGH-SPEED PERMANENT MAGNET MOTOR,” 2025.

[31] A. R. Ansari, “Performance Assessment of Permanent Magnet Brushless DC Motors with Intelligent Controller,” 2022.

[32] S. Pankaj, “Comparative Analysis of MIT Rule and Lyapunov Rule in Model Reference Adaptive Control Scheme,” vol. 2, no. 4, pp. 154–163, 2011.

[33] H. Tahersima, M. Saleh, A. Mesgarisohani, and M. Tahersima, “Design of Stable Model Reference Adaptive System via Lyapunov Rule for Control of a Chemical Reactor,” no. 4, pp. 348–353, 2013.

[34] D. W. Gu, P. H. Petkov, and M. M. Konstantinov, *Advanced Textbooks in Control and Signal Processing with Matlab*. 2005.

[35] P. J. Kennedy, “Proportional , Integral , and Derivative Controller Design Part 2 by”.